ESAIM: M2AN 59 (2025) 3249–3281
https://doi.org/10.1051/m2an/2025072

ESAIM: Mathematical Modelling and Numerical Analysis
www.esaim-m2an.org

EFFICIENT FINITE ELEMENT METHODS FOR SEMICLASSICAL NONLINEAR SCHRÖDINGER EQUATIONS WITH RANDOM POTENTIALS

Panchi Li[1] and Zhiwen Zhang[1,2,*]

Abstract. In this paper, we propose two time-splitting finite element methods to solve the semiclassical nonlinear Schrödinger equation (NLSE) with random potentials. We then introduce a multiscale method to reduce the degrees of freedom in the physical space. We construct multiscale basis functions by solving optimization problems and rigorously analyze the corresponding time-splitting multiscale reduced methods for the semiclassical NLSE with random potentials. We provide the L^2 error estimate of the proposed methods and show that they achieve second-order accuracy in both spatial and temporal spaces and an almost first-order convergence rate in the random space. Additionally, we introduce the proper orthogonal decomposition method to reduce the computational cost of constructing basis functions for solving random NLSEs. Finally, we carry out several 1D and 2D numerical examples to validate the convergence of our methods and investigate wave propagation behaviors in the NLSE with random potentials.

Mathematics Subject Classification. 35Q55, 65M60, 81Q05, 47H40.

Received December 31, 2024. Accepted August 29, 2025.

1. Introduction

The nonlinear Schrödinger equation (NLSE) is a prototypical dispersive nonlinear equation that has been extensively used to study the Bose–Einstein condensation, laser beam propagation in nonlinear optics, particle physics, semi-conductors, superfluids, etc. To accurately and transparently interpret the observations in many experimental situations, a semiclassical treatment is extensively introduced for the underlying quantum mechanical dynamics [45]. For the NLSE, this treatment results a small semiclassical parameter ϵ, and propagations of ϵ-dependent oscillations in both space and time. With a further consideration of random potentials, the interaction of nonlinearity and random effect also poses challenges to understanding complex phenomena, such as localization and delocalization [19, 24, 46, 54] and the soliton propagation [23, 35, 51]. Due to the inherent challenges in studying the underlying model analytically, people devote to developing reliable and efficient numerical approaches to simulate the quantum mechanical dynamics.

In the past decades, many numerical methods have been proposed to solve the NLSEs with deterministic potentials, and recent comparisons can be found in [3, 5, 28]. For the time-dependent NLSE, the implicit Crank–

Keywords and phrases. Semiclassical nonlinear Schrödinger equation, finite element method, multiscale finite element method, random potentials, time-splitting methods.

[1] Department of Mathematics, The University of Hong Kong, Hong Kong, P.R. China.
[2] Materials Innovation Institute for Life Sciences and Energy (MILES), HKU-SIRI, Shenzhen, P.R. China.
*Corresponding author: zhangzw@hku.hk

Nicolson (CN) schemes were extensively used. The CN scheme conserves the mass and energy of the system simultaneously, but it is known for a lower efficiency in handling nonlinearity with the requirement of iteration methods, in which particular time step conditions must be ensured for the stability of the iteration [1,41,52]. To enhance computational efficiency, several promising approaches, including linearized implicit methods [57,62], relaxation methods [9,11] and time-splitting methods [8,10,56], have been proposed. Among these, time-splitting methods exhibit outstanding performance in terms of efficiency since linear equations with constant coefficients are solved at each time step. To reach optimal convergence, time-splitting schemes require enough smoothness on both the potential and the initial condition. For instance, Strang splitting methods require the initial condition to possess H^4 regularity [10]. The low-regularity time-integrator methods [37,47,61] are proposed to alleviate such a constraint. Nevertheless, the available low-regularity time-integrator methods rely on the Fourier discretization in space with a periodical setup, and their integration with finite difference methods (FDM) and finite element methods (FEM) has not been established.

Although the Fourier discretization allows for the approximation error to reach exponential accuracy in space, in the case of non-smooth potentials, the FDM or FEM is recommended, as spectral methods may lose their optimal convergence rate. In this paper, we invest to develop efficient numerical methods based on the FEM. Over the past several decades, to develop efficient FEM methods for partial differential equations, intense research efforts in dimensionality reduction methods by constructing the multiscale reduced basis functions, known as the multiscale finite method (MsFEM), have been invested (see, *e.g.*, [2, 15, 20–22, 26, 31, 49]). Incorporating the local microstructures of the differential operator into the basis functions, MsFEMs capture the large-scale components of the multiscale solution on a coarse mesh without the need to resolve all the small-scale features on a fine mesh.

Recently, the localized orthogonal decomposition (LOD) method [2, 44] has been proposed to approximate the minimizes of the energy [27, 29, 30] and simulate the time-dependent dynamics [18] for the NLSE with deterministic potential, which achieves a superconvergence rate in space. With the random potential further being considered, the time-splitting spectral discretization with the Monte Carlo (MC) sampling [61] and quasi-Monte Carlo (qMC) sampling [60] have been employed for the 1D NLSE. Considering the limitation of the spectral methods, and developing efficient numerical methods in the framework of the FEM, here we combine the time-splitting temporal discretization and a multiscale method to solve the NLSE with random potentials.

In our approaches, the multiscale basis functions are approximated using the finite element basis on a fine mesh, where the coefficients are determined by solving a set of equality-constrained quadratic programs. This idea was motivated by the multiscale method for elliptic problems with random coefficients [32–34], the linear Schrödinger equation with multiscale and random potentials [14], and the Helmholtz equation in random media [42]. We use the multiscale basis functions to discretize the deterministic NLSE that reduces the degrees of freedom (dofs) required for FEM. Meanwhile, for the time-marching, we present two Strang splitting methods. One solves the linear Schrödinger equation using the eigendecomposition method [14] and handles the cubic ordinary differential equation at each time step. This splitting method obviates the requirement of regularity for the potential function. The other is the time-splitting CN method. Meanwhile, the random potential is parameterized using the Karhunen–Loève (KL) expansion method. We employ the qMC method to generate random samples. It is demonstrated that the proposed approaches reach the second-order convergence rate in both time and space, and achieve almost a first-order convergence rate with respect to the sampling number in the random space.

Theoretically, we provide a convergence analysis of the time-splitting FEM (TS-FEM) for the deterministic NLES in Lemma 4.3. Furthermore, we extend this analysis to estimate the time-splitting multiscale method for the NLSEs with random potentials as Theorem 4.3. We remark that the referred multiscale method should be an LOD method, although we use a different approach to construct the multiscale basis. On the other hand, this optimal approach allows us to apply the proper orthogonal decomposition (POD) method, which essentially reduces the computational costs for the construction of the optimal multiscale basis for new qMC samples in a low-dimensional POD basis space. The corresponding method is detailed in Appendix A. Numerically, we verify several theoretical aspects. Using the proposed numerical methods, we investigate wave propagation in

the NLSE with parameterized random potentials in both 1D and 2D physical spaces. We observe the localized phenomena of mass density for the linear cases, whereas the NLSE with strong nonlinearity exhibits significant delocalization.

The rest of the paper is organized as follows. In Section 2, we describe fundamental model problems. In Section 3, we present the spatial discretization methods with time-splitting methods for the deterministic NLSEs. Then, the analysis results are presented in Section 4. Numerical experiments, including 1D and 2D examples, are conducted in Section 5. Finally, conclusions are drawn in Section 6.

2. The semiclassical NLSE with random potentials

We consider the following model problem

$$\begin{cases} i\epsilon\partial_t\psi^\epsilon = -\dfrac{\epsilon^2}{2}\Delta\psi^\epsilon + v(\boldsymbol{x},\omega)\psi^\epsilon + \lambda|\psi^\epsilon|^2\psi^\epsilon, \quad \boldsymbol{x}\in\mathcal{D}, \quad \omega\in\Omega, \quad t\in(0,T], \\ \psi^\epsilon|_{t=0} = \psi_{\text{in}}(\boldsymbol{x}), \end{cases} \tag{2.1}$$

where $0 < \epsilon \ll 1$ is an effective Planck constant, $\mathcal{D} = \mathbb{T}^d (d = 1, 2, 3)$ denotes the torus, $\omega \in \Omega$ is the random sample with Ω being the random space, T is the terminal time, $\psi_{\text{in}}(\boldsymbol{x})$ denotes the initial state, $v(\boldsymbol{x},\omega)$ is a given random potential, and λ (≥ 0) is the nonlinearity coefficient. Physically, $|\psi^\epsilon|^2$ denotes the mass density and the system's total mass $m_T = \int_{\mathcal{D}} |\psi_{\text{in}}|^2 \,\mathrm{d}\boldsymbol{x}$ is conserved by (2.1). Note that the wave function $\psi^\epsilon : [0,T]\times\mathcal{D}\times\Omega \to \mathbb{C}$, and the function space $H^1_P(\mathcal{D}) = H^1_P(\mathcal{D},\mathbb{C})$, in which the functions are periodic over domain $\mathcal{D}$. The inner product is defined as $(v,w) = \int_{\mathcal{D}} v\overline{w}\,\mathrm{d}\boldsymbol{x}$ with $\overline{w}$ denoting the complex-conjugate of w, and the spatial L^2 norm is $\|w\|^2 = \||w|\|^2 = (w,w)$. Furthermore, let $D^{\boldsymbol{\sigma}} = \partial^{s_1}_{x_1}\cdots\partial^{s_d}_{x_d}$ denote the spatial derivative with $|\boldsymbol{\sigma}| = s_1 + \cdots + s_d$. Then, the H^k norm is denoted by $\|\cdot\|_{H^k}$ with $\|\cdot\|^2_{H^k} = \|\cdot\|^2 + \sum_{1\leq|\boldsymbol{\sigma}|\leq k}\|D^{\boldsymbol{\sigma}}\cdot\|^2$. In particular, the spatial L^∞ norm is defined by $\|\cdot\|_\infty = \operatorname{ess\,sup}_{\boldsymbol{x}\in\mathcal{D}}|\cdot|$.

We denote the Hamiltonian operator $\mathcal{H}$ of the NLSE

$$\mathcal{H}(\cdot) = -\frac{\epsilon^2}{2}\Delta(\cdot) + v(\cdot) + \lambda|\cdot|^2(\cdot). \tag{2.2}$$

Since the Hamiltonian operator is not explicitly dependent on time and the commutator $[\mathcal{H},\mathcal{H}] = 0$, the energy of the system,

$$E(t) = (\mathcal{H}\psi^\epsilon,\psi^\epsilon) = \frac{\epsilon^2}{2}\|\nabla\psi^\epsilon\|^2 + (v(\boldsymbol{x},\omega),|\psi^\epsilon|^2) + \frac{\lambda}{2}\|\psi^\epsilon\|^4_{L^4}, \tag{2.3}$$

remains unchanged as time evolves. We assume $E(t) = E_0 < \infty$ for all $t > 0$.

Assumption 2.1. *We assume that the potential $v(\boldsymbol{x},\omega)$ is bounded in $L^\infty(\Omega;H^s)$ with $0 \leq s \leq 2$. More precisely, for every $\omega\in\Omega$, the bound of $\|v(\boldsymbol{x},\omega)\|_\infty$ satisfies*

$$H^2 \lesssim \frac{\epsilon^2}{\|v(\boldsymbol{x},\omega)\|_\infty}, \tag{2.4}$$

where $\lesssim$ means bounded by a constant and H, which will be defined later, is the coarse mesh size of the MsFEM.

We first consider the deterministic potential, *i.e.*, $v(\boldsymbol{x},\omega) = v(\boldsymbol{x})$. Assume that there exists a finite time T such that $\psi^\epsilon \in L^\infty([0,T];H^4)\cap L^1([0,T];H^2)$ and by Sobolev embedding theorem, we have $\|\psi^\epsilon\|_\infty \leq C\|\psi^\epsilon\|_{H^2}$ for all $t\in[0,T]$ and $d\leq 3$. Hence, the bonded assumption of $\|\psi^\epsilon\|_\infty$ implies that ψ^ϵ is bounded in the L^∞ sense in both time and space. Apart from this, unless specially stated, the norms should be with respect to the space. Besides, here we directly assume that the solution of (2.1) exists and is unique in a finite time. We refer to a detailed discussion on the existence and uniqueness of the solution in [29] and the references therein. In the sequel, we will use a uniform constant C to denote all the controllable constants that are independent of ϵ for simplicity of notation.

Lemma 2.1. *Assume $v(\boldsymbol{x},\omega)=v(\boldsymbol{x})$ in (2.1) and let ψ^ϵ be the solution of the counterpart system. Assume $\psi^\epsilon\in L^\infty([0,T];H^4)\cap L^1([0,T];H^2)$. If $\partial_t\psi^\epsilon(t)\in H^s$ with $s=0,1,2$ for all $t\in[0,T]$, there exists a constant $C_{\lambda,\epsilon}$ such that*

$$\|\partial_t\psi^\epsilon\|_{H^s}\le C_{\lambda,\epsilon}, \tag{2.5}$$

where $C_{\lambda,\epsilon}$ mainly depends on ϵ and λ. In particular, for $d=3$ and $s=1,2$, we have a compact formulate

$$\|\partial_t\nabla^s\psi^\epsilon\|\le\left(\frac{\|\nabla v\|_\infty+C\lambda\|\nabla^{s+1}\psi^\epsilon\|}{\epsilon}\right)\|\partial_t\nabla^{s-1}\psi^\epsilon\|\exp\left(\frac{C\lambda T(\|\nabla^2\psi^\epsilon\|+\|\psi^\epsilon\|_\infty^2)}{\epsilon}\right),$$

where

$$\|\partial_t\psi^\epsilon\|\le\frac{C}{\epsilon}\exp\left(\frac{2\lambda T\|\psi^\epsilon\|_\infty^2}{\epsilon}\right). \tag{2.6}$$

The proof is detailed in Appendix B, in which the constant $C_{\lambda,\epsilon}$ can be calculated. Note that for $\lambda=0$, the above result can degenerate to the estimate of the linear Schrödinger equation as in [6,59].

Next, we assume that $v(\boldsymbol{x},\omega)$ is a second-order random field, *i.e.*, $\mathbb{E}[|v(\boldsymbol{x},\omega)|^2]<\infty$, with a mean value $\mathbb{E}[v(\boldsymbol{x},\omega)]=v(\boldsymbol{x})$ and a covariance kernel denoted by $C(\boldsymbol{x},\boldsymbol{y})$. In this study, we adopt the covariance kernel

$$C(\boldsymbol{x},\boldsymbol{y})=\sigma^2\exp\left(-\sum_{i=1}^d\frac{|x_i-y_j|^2}{2l_i^2}\right), \tag{2.7}$$

where σ is a constant and l_i denotes the correlation lengths in each dimension. Moreover, we assume that the random potential is almost surely bounded. Using the KL expansion method [36,40], random potentials take the form

$$v(\boldsymbol{x},\omega)=\bar v(\boldsymbol{x})+\sum_{j=1}^\infty\sqrt{\lambda_j}\xi_j(\omega)v_j(\boldsymbol{x}), \tag{2.8}$$

where $\xi_i(\omega)$ represents mean-zero and uncorrelated random variables, and $\{\lambda_i,v_i(\boldsymbol{x})\}$ are the eigenpairs of the covariance kernel $C(\boldsymbol{x},\boldsymbol{y})$. The eigenvalues are sorted in descending order and the decay rate depends on the regularity of the covariance kernel [53]. Hence the random potential can be parameterized by the truncated form

$$v_m(\boldsymbol{x},\omega)=\bar v(\boldsymbol{x})+\sum_{j=1}^m\sqrt{\lambda_j}\xi_j(\omega)v_j(\boldsymbol{x}). \tag{2.9}$$

Once the parameterized form of the random potential is defined, the corresponding wave function ψ_m^ϵ satisfies

$$\begin{cases} i\epsilon\partial_t\psi_m^\epsilon=-\dfrac{\epsilon^2}{2}\Delta\psi_m^\epsilon+v_m(\boldsymbol{x},\omega)\psi_m^\epsilon+\lambda|\psi_m^\epsilon|^2\psi_m^\epsilon, \quad \boldsymbol{x}\in\mathcal{D},\omega\in\Omega,t\in(0,T],\\ \psi_m^\epsilon(t=0)=\psi_{\text{in}}. \end{cases} \tag{2.10}$$

The error $|v_m(\boldsymbol{x},\omega)-v(\boldsymbol{x},\omega)|$ depends on the regularity of eigenfunctions and the decay rate of eigenvalues. We make the following assumption for the parameterized random potentials, which ensures that the random problem is well-posed, and allows us carry out a rigorous analysis for the truncation error. In particular, here we assume that the random potential is almost surely bounded over the domain $\mathcal{D}$, and the KL modes satisfy:

Assumption 2.2. (1) *In the KL expansion (2.9), assume that there exist constants $C>0$ and $\Theta>1$ such that $\lambda_j\le Cj^{-\Theta}$ for all $j\ge1$.*

(2) *The eigenfunctions $v_j(\boldsymbol{x})$ are continuous and there exist constants $C>0$ and $0\le\eta\le\frac{\Theta-1}{2\Theta}$ such that $\|v_j\|_{H^2}\le C\lambda_j^{-\eta}$ for all $j\ge1$.*

(3) *Assume that the parameterized potential v_m satisfies*

$$\|v - v_m\|_\infty \le Cm^{-\chi}, \quad \sum_{j=1}^{\infty}\Big(\sqrt{\lambda_j}\|v_j\|_{H^2}\Big)^p < \infty,$$

for some positive constants C and χ, and $p \in (0,1]$.

In [60], the authors provide the $L^\infty([0,T],H^1)$ error between wave functions to (2.1) and (2.10) for the 1D case. Here we get a similar result for the L^2 error between the wave functions for $d \le 3$.

Lemma 2.2. *For every $\omega \in \Omega$, the error between wave functions to (2.1) and (2.10) satisfies*

$$\|\psi_m^\epsilon - \psi^\epsilon\| \le \frac{C\|v_m - v\|_\infty}{\epsilon}\exp\Big(\frac{4T\lambda}{\epsilon}\|\psi^\epsilon\|_\infty\|\psi_m^\epsilon\|_\infty\Big), \tag{2.11}$$

where C is independent of ϵ.

Proof. Define $\delta\psi = \psi_m^\epsilon - \psi^\epsilon$ and it satisfies

$$i\epsilon\partial_t\delta\psi = -\frac{\epsilon^2}{2}\Delta\delta\psi + v_m\delta\psi + (v_m - v)\psi^\epsilon + \lambda\Big(|\psi_m^\epsilon|^2\psi_m^\epsilon - |\psi^\epsilon|^2\psi^\epsilon\Big) \tag{2.12}$$

with the initial condition $\delta\psi(t=0) = 0$. For the nonlinear term, we have

$$|\psi_m^\epsilon|^2\psi_m^\epsilon - |\psi^\epsilon|^2\psi^\epsilon = \big|\psi_m^\epsilon|^2\delta\psi + \psi^\epsilon\psi_m^\epsilon\delta\bar{\psi} + \big|\psi^\epsilon|^2\delta\psi.$$

Taking the inner product of (2.12) with $\delta\psi$ yields

$$\begin{aligned} i\epsilon(\partial_t\delta\psi,\delta\psi) = {}& \frac{\epsilon^2}{2}(\nabla\delta\psi,\nabla\delta\psi) + (v_m\delta\psi,\delta\psi) + ((v_m - v)\psi^\epsilon,\delta\psi) \\ & + \lambda\Big(|\psi_m^\epsilon|^2\delta\psi,\delta\psi\Big) + \lambda\big(\psi^\epsilon\psi_m^\epsilon\delta\bar{\psi},\delta\psi\big) + \lambda\Big(|\psi^\epsilon|^2\delta\psi,\delta\psi\Big), \end{aligned}$$

which infers

$$\frac{i\epsilon}{2}\,\mathrm{d}_t\|\delta\psi\|^2 = ((v_m - v)\psi^\epsilon,\delta\psi) - \big((v_m - v)\bar{\psi}^\epsilon,\delta\bar{\psi}\big) + \lambda\big(\big(\psi^\epsilon\delta\bar{\psi},\bar{\psi}_m^\epsilon\delta\psi\big) - \big(\bar{\psi}^\epsilon\delta\psi,\psi_m^\epsilon\delta\bar{\psi}\big)\big).$$

We further get

$$\begin{aligned} \mathrm{d}_t\|\delta\psi\|^2 &\le \frac{4\|v_m - v\|_\infty}{\epsilon}\int_{\mathcal{D}}|\psi^\epsilon||\delta\psi|\,\mathrm{d}\boldsymbol{x} + \frac{4\lambda}{\epsilon}\int_{\mathcal{D}}|\psi^\epsilon\delta\psi||\psi_m^\epsilon\delta\psi|\,\mathrm{d}\boldsymbol{x} \\ &\le \frac{4\|v_m - v\|_\infty}{\epsilon}\|\psi^\epsilon\|\|\delta\psi\| + \frac{4\lambda}{\epsilon}\|\psi^\epsilon\|_\infty\|\psi_m^\epsilon\|_\infty\|\delta\psi\|^2. \end{aligned}$$

Owing to the $L^\infty([0,T]\times\Omega;H^s)$ bound of both ψ^ϵ and ψ_m^ϵ, an application of Gronwall inequality yields

$$\|\delta\psi\| \le \frac{4T\|v_m - v\|_\infty}{\epsilon}\exp\Big(\frac{4T\lambda}{\epsilon}\|\psi^\epsilon\|_\infty\|\psi_m^\epsilon\|_\infty\Big).$$

□

Owing to the assumption $\|v_m - v\|_\infty \le Cm^{-\chi}$, this lemma implies that $\psi_m^\epsilon \to \psi^\epsilon$ as $m \to \infty$.

3. Numerical methods

Consider the regular mesh $\mathcal{T}_h$ of $\mathcal{D}$. The standard P_1 finite element space on the mesh $\mathcal{T}_h$ is given by $P_1(\mathcal{T}_h) = \{v \in L^2(\bar{\mathcal{D}})|$ for all $K \in \mathcal{T}_h, v|_K$ is a polynomial of total degree $\leq 1\}$. Let $\mathcal{T}_H$ denote the coarse mesh with mesh size H, and then the $H_P^1(\mathcal{D})$-conforming finite element spaces are $V_h = P_1(\mathcal{T}_h) \cap H_P^1(\mathcal{D})$ and $V_H = P_1(\mathcal{T}_H) \cap H_P^1(\mathcal{D})$. Denote $V_h = span\{\phi_1^h, \cdots, \phi_{N_h}^h\}$ and $V_H = span\{\phi_1^H, \cdots, \phi_{N_H}^H\}$, where N_h and N_H are the number of vertices of the fine mesh and the coarse mesh, respectively. The wave function is approximated by $\psi_h^\epsilon(t, \boldsymbol{x}) = \sum_p^{N_h} U_p(t)\phi_p^h(\boldsymbol{x})$ on the fine mesh, where $U_p(t) \in \mathbb{C}, p = 1, \cdots, N_h$ and $t \in [0, T]$.

3.1. TS-FEM for the NLSE

We adopt Strang splitting methods for time-stepping. The NLSE is rewritten to

$$i\epsilon\partial_t\psi^\epsilon = (\mathcal{L}_1 + \mathcal{L}_2)\psi^\epsilon, \tag{3.1}$$

and its exact solution has the form $\psi^\epsilon(t) = S^t\psi_{\text{in}}$, where $S^t = \exp(-i(\mathcal{L}_1 + \mathcal{L}_2)t/\epsilon)$. To efficiently handle the nonlinear term, we present two approaches as follows, both of which require solving linear equations:

(1) Option 1,

$$\mathcal{L}_1(\cdot) = -\frac{\epsilon^2}{2}\Delta(\cdot) + v(\cdot), \quad \mathcal{L}_2(\cdot) = \lambda|\cdot|^2(\cdot). \tag{3.2}$$

(2) Option 2,

$$\mathcal{L}_1(\cdot) = -\frac{\epsilon^2}{2}\Delta(\cdot), \quad \mathcal{L}_2(\cdot) = v(\cdot) + \lambda|\cdot|^2(\cdot). \tag{3.3}$$

Computing the commutator $[\mathcal{L}_1, \mathcal{L}_2] = \mathcal{L}_1\mathcal{L}_2 - \mathcal{L}_2\mathcal{L}_1$ shows that the regularity of potential $v \in C^2(\mathcal{D})$ is required for Option 2, whereas Option 1 does not need this condition.

From t_n to t_{n+1}, the Strang splitting yields

$$\psi^{\epsilon,n+1} := \mathcal{L}\psi^{\epsilon,n} = \exp\left(-\frac{i\Delta t}{2\epsilon}\mathcal{L}_2(\cdot)\right) \circ \exp\left(-\frac{i\Delta t}{\epsilon}\mathcal{L}_1\right) \exp\left(-\frac{i\Delta t}{2\epsilon}\mathcal{L}_2(\cdot)\right) \circ \psi^{\epsilon,n}. \tag{3.4}$$

This formulation can be written as

$$\psi^{\epsilon,n+1} = \exp\left(-\frac{i\Delta t}{\epsilon}(\mathcal{L}_1 + \mathcal{L}_2(\psi^{\epsilon,n}))\right)\psi^{\epsilon,n} + \mathcal{R}_1^n. \tag{3.5}$$

By the Taylor expansion, we have $\|\mathcal{R}_1^n\| = \mathcal{O}(\frac{\Delta t^3}{\epsilon^3})$. Furthermore, we define the n-fold composition

$$\psi^{\epsilon,n} = \mathcal{L}^n\psi_{\text{in}} = \underbrace{\mathcal{L}(\Delta t, \cdot) \circ \cdots \circ \mathcal{L}(\Delta t, \cdot)}_{n \text{ times}}\psi_{\text{in}}. \tag{3.6}$$

And for the finite element discretization, define

$$i\epsilon(\partial_t\psi^\epsilon, \phi) = a(\psi^\epsilon, \phi), \quad \forall\phi \in H_P^1(\mathcal{D}),$$

where $a(\psi^\epsilon, \phi)$ is determined by the option of $\mathcal{L}_1$. For example, setting $\mathcal{L}_1 = -\frac{\epsilon^2}{2}\Delta + v$, we have $a(\psi^\epsilon, \phi) = \frac{\epsilon^2}{2}(\nabla\psi^\epsilon, \nabla\phi) + (v\psi^\epsilon, \phi)$ and the Galerkin equations

$$i\epsilon\sum_p \mathrm{d}_t U_p(t)\big(\phi_p^h, \phi_q^h\big) = \frac{\epsilon^2}{2}\sum_p U_p(t)\big(\nabla\phi_p^h, \nabla\phi_q^h\big) + \sum_p U_p(t)\big(v\phi_p^h, \phi_q^h\big) \tag{3.7}$$

with $q = 1, \cdots, N_h$. Its matrix form is

$$i\epsilon M^h\,\mathrm{d}_t U(t) = \left(\frac{\epsilon^2}{2}S^h + V^h\right)U(t), \tag{3.8}$$

where $U(t)$ is a vector with $U(t) = (U_1(t), \cdots, U_{N_h}(t))^T$, $M^h = [M^h_{pq}]$ is the mass matrix with $M^h_{pq} = (\phi^h_p, \phi^h_q)$, $S^h = [S^h_{pq}]$ is the stiff matrix with $S^h_{pq} = (\nabla\phi^h_p, \nabla\phi^h_q)$, and $V^h = [V^h_{pq}]$ is the potential matrix with $V^h_{pq} = (v\phi^h_p, \phi^h_q)$.

We now present the formal TS-FEM methods for the deterministic NLSE. The first one is the discretized counterpart of Option 1:

$$\begin{aligned}
\tilde{U}^n &= \exp\left(-\frac{i\lambda\Delta t}{2\epsilon}|U^n|^2\right)U^n,\\
\tilde{U}^{n+1} &= P\exp\left(-\frac{i\Delta t}{\epsilon}\Lambda\right)(P^{-1}\tilde{U}^n),\\
U^{n+1} &= \exp\left(-\frac{i\lambda\Delta t}{2\epsilon}\left|\tilde{U}^{n+1}\right|^2\right)\tilde{U}^{n+1},
\end{aligned} \tag{3.9}$$

where $(M^h)^{-1}(\frac{\epsilon^2}{2}S^h + V^h) = P\Lambda P^{-1}$ with $\exp(-i\Delta t\Lambda/\epsilon)$ being a diagonal matrix, and $U^n = U(t_n)$. We call it **SI** in the remainder of this paper. Owing to the application of the eigendecomposition method [14], the error in time is mainly contributed by the time-splitting manner. Meanwhile, this scheme does not require time step size $\Delta t = o(\epsilon)$, although the full linear semiclassical Schrödinger equation must be solved.

Option 2 has been extensively used in previous works, such as [7, 8]. In the FEM framework, it solves the NLES in the following procedures:

$$\begin{aligned}
\tilde{U}^n &= \exp\left(-\frac{i\Delta t}{2\epsilon}\left(v + \lambda|U^n|^2\right)\right)U^n,\\
iM^h\left(\frac{\tilde{U}^{n+1} - \tilde{U}^n}{\Delta t}\right) &= \frac{\epsilon}{2}S^h\left(\frac{\tilde{U}^{n+1} + \tilde{U}^n}{2}\right),\\
U^{n+1} &= \exp\left(-\frac{i\Delta t}{2\epsilon}\left(v + \lambda\left|\tilde{U}^{n+1}\right|^2\right)\right)\tilde{U}^{n+1}.
\end{aligned} \tag{3.10}$$

This method requires the mesh size $h = \mathcal{O}(\epsilon)$ and time step size $\Delta t = \mathcal{O}(\epsilon)$ [8], and we call it **SII** in the remaining part of this paper.

Remark 3.1. In the discrete level, owing to $\phi^h_p(\mathbf{x}_q) = \delta_{pq}$, we have $|\psi_h(x_p)|^2 = |U_p|^2$. This implies that at all spatial nodes, the finite element solution can be obtain using the algebraic forms $\exp\left(-\frac{i\lambda\Delta t}{2\epsilon}(\cdot)\right)$. Nevertheless, we must note that an approximation error in space is introduced in the first and third steps of both (3.9) and (3.10).

Denote L the discretized counterpart of $\mathcal{L}$, and similarly, L_1 and L_2 their respective discretized versions. Denote $\psi^{\epsilon,n}_h = \sum_{p=1}^{N_h} U^n_p\phi^h_p$, and for simplicity we employ a formal notation for the n-fold composition

$$\psi^{\epsilon,n}_h = L^n\psi^0_h = \underbrace{L(\Delta t,\cdot)\circ\cdots\circ L(\Delta t,\cdot)}_{n \text{ times}}\psi^0_h, \tag{3.11}$$

where $\psi^0_h = R_h\psi_{\text{in}}$ with R_h being the Ritz projection operator.

3.2. The spatial discretization for the deterministic NLSE

Instead of the FEM, we construct the multiscale basis functions to reduce dofs in computations. The P_1 FEM basis functions on both the coarse mesh $\mathcal{T}_H$ and fine mesh $\mathcal{T}_h$ are required simultaneously. To describe the localized property of multiscale basis functions, we define a series of nodal patches $\{D_\ell\}$ associated with $\boldsymbol{x}_p \in \mathcal{N}_H$ as

$$D_0(\boldsymbol{x}_p) := \text{supp}\{\phi_p\} = \cup\{K \in \mathcal{T}_H \mid \boldsymbol{x}_p \in K\},$$

$$D_\ell := \cup\{K \in \mathcal{T}_H \mid K \cap \overline{D_{\ell-1}} \neq \emptyset\}, \quad \ell = 1, 2, \cdots.$$

The multiscale basis function at $\boldsymbol{x}_p$ is the solution of the following optimization problem

$$\arg \min_{\phi \in H_P^1(\mathcal{D})} a(\phi, \phi), \tag{3.12}$$

$$\text{s.t.} \int_{\mathcal{D}} \phi \phi_q^H \, \mathrm{d}\boldsymbol{x} = \lambda(H)\delta_{pq}, \quad q = 1, \cdots, N_H, \tag{3.13}$$

where $a(\phi, \phi) = \frac{\epsilon^2}{2}(\nabla\phi, \nabla\phi) + (v\phi, \phi)$, and $\lambda(H) = 1$ in the previous work [12–14,34,38]. Note that the localized constraint is not considered in the optimal problems, thus we obtain the global basis functions.

Remark 3.2. The referred dofs of the global multiscale basis depend on the fine mesh, which implies that for high-dimensional problems, it suffers from both time and memory consumption. Therefore, the localized multiscale basis is commonly employed in various practices. The localization shall introduce a localization error, such as the LOD method [44]. In Appendix A, we present a reduction method that combines the POD method with the multiscale method, and then the dofs referred to in the construction of basis functions only rely on the dimensions of the POD basis and are independent of the fine mesh. Therefore, the localization error may be ignored to a certain extent in our methods, even though we can still employ the proper localization for high-dimensional problems.

In this work, we set $\lambda(H) = (1, \phi_q^H)$, and it can be computed explicitly. To explain this setup, we introduce the weighted Clément-type quasi-interpolation operator [26]

$$I_H : H_P^1(\mathcal{D}) \to V_H, \quad f \mapsto I_H(f) := \sum_p \frac{(f, \phi_p^H)}{(1, \phi_p^H)} \phi_p^H. \tag{3.14}$$

The high-resolution finite element space $V_h = V_H \oplus W_h$, where W_h is the kernel space of I_H. And for all $f \in H_P^1 \cap H^2$, it holds [43]

$$\|f - I_H(f)\| \leq H^2 \|f\|_{H^2}. \tag{3.15}$$

In the multiscale basis space, the wave function ψ^ϵ is approximated as

$$\psi^\epsilon(\boldsymbol{x}) \approx \sum_{p=1}^{N_H} \hat{U}_p \phi_p. \tag{3.16}$$

It can be projected onto the coarse mesh through

$$I_H(\psi^\epsilon) = \sum_{p=1}^{N_H} \frac{\left(\sum_{q=1}^{N_H} \hat{U}_q \phi_q, \phi_p^H\right)}{(1, \phi_p^H)} \phi_p^H = \sum_{p=1}^{N_H} \frac{\lambda(H)\hat{U}_p}{(1, \phi_p^H)} \phi_p^H.$$

If ψ^ϵ is continuous at $\boldsymbol{x}_p$, the above formula indicates that

$$\psi^\epsilon(\boldsymbol{x}_p) \approx \frac{\lambda(H)\hat{U}_p}{(1, \phi_p^H)}.$$

Let $\lambda(H) = 1$, and we can see that it holds $\psi^\epsilon(\boldsymbol{x}_p) \approx \hat{U}_p/(1, \phi_p^H)$. Define $\hat{\phi}_p = (1, \phi_p^H)\phi_p$, where $\hat{\phi}_p$ is independent of the mesh size H. Then, (3.16) can be rewritten to

$$\psi^\epsilon(\boldsymbol{x}) \approx \sum_{p=1}^{N_H} \psi^\epsilon(\boldsymbol{x}_p)(1, \phi_p^H)\phi_p = \sum_{p=1}^{N_H} \psi^\epsilon(\boldsymbol{x}_p)\hat{\phi}_p. \tag{3.17}$$

Note that $\hat{\phi}_p$ is still the multiscale basis function at $\boldsymbol{x}_p$. We consider the following two equations

$$i\epsilon \sum_{p=1}^{N_H} (\phi_p, \phi_q)\, \mathrm{d}_t \hat{U}_p = \sum_{p=1}^{N_H} (\mathcal{H}\phi_p, \phi_q)\hat{U}_p \tag{3.18}$$

and

$$i\epsilon \sum_{p=1}^{N_H} \left(\hat{\phi}_p, \hat{\phi}_q\right) \mathrm{d}_t \hat{U}_p = \sum_{p=1}^{N_H} \left(\mathcal{H}\hat{\phi}_p, \hat{\phi}_q\right)\hat{U}_p. \tag{3.19}$$

If $\lambda = 0$, the two equations have the same solution with a given initial condition, while for $\lambda \neq 0$, the factor $(1, \phi_p^H)$ in the basis functions cannot be eliminated in both sides of (3.19), and the two equations give different solutions. This issue is addressed by the setup $\lambda(H) = (1, \phi_p^H)$.

Solving the optimal problems (3.13), we get

$$\phi_p = \sum_{s=1}^{N_h} c_p^s \phi_s^h, \quad p = 1, \cdots, N_H.$$

Define $V_{ms} = span\{\phi_1, \cdots, \phi_{N_H}\}$, and it holds true that $V_{ms} \subset V_h$. Hence, the solution of optimal problems defines a mapping $\mathcal{C} : V_h \mapsto V_{ms}$. On the other hand, the solution on the fine mesh can be reconstructed utilizing this linear mapping, which is essential in the formulation of the cubic nonlinear matrix. Note that the factor $\lambda(H)$ is a rescaling factor, and it does not change the basis function space. Thus we have the following propositions.

Proposition 3.1 ([59], Lem. 3.2)**.** *For all $\phi \in V_{ms}$ and $w \in W_h$, $a(\phi, w) = 0$ and $V_h = V_{ms} \oplus W_h$.*

Proof. As the same procedures in [59], we directly obtain $a(f, w) = 0, \forall f \in V_{ms}, w \in W_h$. For any $f \in V_h$, define

$$f^* = \sum_{p=1}^{N_H} \frac{(f, \phi_p^H)}{(1, \phi_p^H)} \phi_p.$$

Then $f^* \in V_{ms}$ and $(f - f^*, \phi_p^H) = 0$ for $p = 1, \cdots, N_H$. Thus $f - f^* \in W_h$ and we get the decomposition $V_h = V_{ms} \oplus W_h$. □

Due to $V_h = V_{ms} \oplus W_h$, W_h is also the kernel space of the mapping $\mathcal{C}$. Furthermore, combining an iterative Caccioppoli-type argument [32, 38, 48, 50] and some refined assumption for the potential, and the multiscale finite element basis functions have the following exponential decaying property.

Proposition 3.2 ([59], Thm. 3.2)**.** *Under Assumption 2.1 with a resolution constant as in [59], there exists a constant $\beta \in (0, 1)$ independent of H and ϵ, such that*

$$\|\nabla \phi_p\|_{L^2(\mathcal{D}\setminus D_\ell)} \leq \beta^\ell \|\nabla \phi_p\|, \tag{3.20}$$

for all $p = 1, \cdots, N_H$.

Once the multiscale basis space being prepared, the weak form of the full NLSE is discretized as

$$\begin{aligned} i\epsilon \left(\sum_{p=1}^{N_H} \sum_{s=1}^{N_h} \mathrm{d}_t \hat{U}_p c_p^s \phi_s^h, \sum_{s=1}^{N_h} c_l^s \phi_s^h \right) &= \frac{\epsilon^2}{2} \left(\sum_{p=1}^{N_H} \sum_{s=1}^{N_h} \hat{U}_p c_p^s \nabla \phi_s^h, \sum_{s=1}^{N_h} c_l^s \nabla \phi_s^h \right) \\ &+ \lambda \left(\left| \sum_{p=1}^{N_H} \sum_{s=1}^{N_h} \hat{U}_p c_p^s \phi_s^h \right|^2 \sum_{p=1}^{N_H} \sum_{s=1}^{N_h} \hat{U}_p c_p^s \phi_s^h, \sum_{s=1}^{N_h} c_l^s \phi_s^h \right) \end{aligned} \tag{3.21}$$

for all $l = 1, \cdots, N_H$. The stiff matrix and mass matrix constructed by the multiscale basis functions satisfy $M^{ms} = \mathcal{C}^T M^h \mathcal{C}$ and $S^{ms} = \mathcal{C}^T S^h \mathcal{C}$. For the nonlinear term, the solution on the fine mesh is reconstructed by $\mathcal{C}\hat{U}$, and we then get the similar form $N^{ms} = \mathcal{C}^T N^h \mathcal{C}$. The construction of N^h suffers from heavy computation, especially for high-dimensional problems. The application of time-splitting methods can avoid this issue. Thus, we only need to solve linear equations at each time step, achieving high efficiency.

According to (3.16) and (3.17), the numerical solution on the coarse mesh can be denoted by $\{\hat{U}_p(t)\}_{p=1}^{N_H}$, while on the fine mesh, it is denoted by $\{\sum_{p=1}^{N_H} \hat{U}_p(t) c_p^s\}_{s=1}^{N_h}$. For the sake of clarity, in the sequel, we denote the ψ_h^ϵ the classical FEM solution, and ψ_H^ϵ and $\psi_{H,h}^\epsilon$ the numerical solution constructed by the multiscale basis functions on the coarse mesh and fine mesh, respectively.

4. Convergence analysis

4.1. Convergence analysis of the TS-FEM

In this part, the **SI** is mainly considered, and the L^2 error will be estimated. We start the convergence analysis from the temporal error estimate at the initial time step.

Lemma 4.1. *If $\psi_{\text{in}} \in H^4$, the error at the initial time step is bounded in the L^2 norm by*

$$\left\|\psi^\epsilon(\Delta t) - \psi^{\epsilon,1}\right\| = \left\|S^{\Delta t}\psi_{\text{in}} - \mathcal{L}(\Delta t)\psi_{\text{in}}\right\| \le C\|\psi_{\text{in}}\|_{H^4}\frac{\Delta t^3}{\epsilon^3},$$

where C is a constant independent of both ϵ and H.

Proof. According to (3.5), we have

$$\begin{aligned}
\psi^{\epsilon,1} &= \exp\left(-\frac{i\Delta t}{2\epsilon}\mathcal{L}_2(\hat{\psi}) - \frac{i\Delta t}{\epsilon}\mathcal{L}_1 - \frac{i\Delta t}{2\epsilon}\mathcal{L}_2(\psi_{\text{in}}^\epsilon)\right)\psi_{\text{in}}^\epsilon \\
&= \exp\left(-\frac{i\Delta t}{2\epsilon}\left(\mathcal{L}_2(\psi_{\text{in}}^\epsilon) + \mathcal{O}\left(\frac{\Delta t^2}{\epsilon^2}\right)\right) - \frac{i\Delta t}{\epsilon}\mathcal{L}_1 - \frac{i\Delta t}{2\epsilon}\mathcal{L}_2(\psi_{\text{in}}^\epsilon)\right)\psi_{\text{in}}^\epsilon \\
&= \exp\left(-\frac{i\Delta t}{\epsilon}\mathcal{L}_1 - \frac{i\Delta t}{\epsilon}\mathcal{L}_2(\psi_{\text{in}}^\epsilon)\right)\exp\left(-\frac{\Delta t^3}{\epsilon^3}\Gamma(2\mathcal{L}_1 + \mathcal{L}_2)^2\right)\psi_{\text{in}}^\epsilon,
\end{aligned}$$

where Γ depends on the form of $\mathcal{L}_2$. Use the expansion

$$\exp\left(-\frac{\Delta t^3}{\epsilon^3}\Gamma(2\mathcal{L}_1 + \mathcal{L}_2)^2\right) = I - \frac{\Delta t^3}{\epsilon^3}\Gamma(2\mathcal{L}_1 + \mathcal{L}_2)^2 + \mathcal{O}\left(\frac{\Delta t^6}{\epsilon^6}\right)$$

and the dominant reminder has the form

$$\mathcal{R}_1^0 = -\frac{\Delta t^3}{\epsilon^3}\Gamma(2\mathcal{L}_1 + \mathcal{L}_2)^2\psi_{\text{in}}^\epsilon.$$

Since the exact solution at $t = \Delta t$ is given by

$$\psi^\epsilon(\Delta t) = S^{\Delta t}\psi_{\text{in}}^\epsilon = \exp\left(-\frac{i\Delta t}{\epsilon}(\mathcal{L}_1 + \mathcal{L}_2(\psi_{\text{in}}^\epsilon))\right)\psi_{\text{in}}^\epsilon.$$

There exists a constant such that

$$\left\|\psi^\epsilon(\Delta t) - \psi^{\epsilon,1}\right\| \le C\|\psi_{\text{in}}^\epsilon\|_{H^4}\frac{\Delta t^3}{\epsilon^3}.$$

□

In turn, we prove the stability of the Strang splitting operator. Due to $\exp(-\frac{i\mathcal{L}_1 t}{\epsilon})$ being unitary, for any f_1, $f_2 \in H^2$, we have

$$\left\|\exp\left(-\frac{i\mathcal{L}_1 t}{\epsilon}\right) f_1 - \exp\left(-\frac{i\mathcal{L}_1 t}{\epsilon}\right) f_2\right\| = \left\|\exp\left(-\frac{i\mathcal{L}_1 t}{\epsilon}\right)(f_1 - f_2)\right\| = \|f_1 - f_2\|.$$

Define $F(\psi) = -i\mathcal{L}_2(\psi)\psi$, the splitting solution for $\mathcal{L}_2$ is solved by the equation $\epsilon\partial_t\psi - F(\psi) = 0$. The nonlinear flow solved from this equation has the form

$$Y^t\psi = \psi + \frac{1}{\epsilon}\int_0^t F(Y^s\psi)\,\mathrm{d}s, \tag{4.1}$$

where the flow Y^t is defined as

$$\psi(t,\cdot) = Y^t\psi(0,\cdot) = \psi(0,\cdot)\exp\left(-\frac{i}{\epsilon}\int_0^t \mathcal{L}_2(\psi)\,\mathrm{d}s\right).$$

Assume that F is Lipschitz with a Lipschitz constant M, and repeat the proof in [10]. For all f_1, $f_2 \in L^2$, there exists a constant that depends on F such that for all $0 \le \tau \le 1$

$$\begin{aligned}\|Y^\tau f_1 - Y^\tau f_2\| &\le \|f_1 - f_2\| + \frac{1}{\epsilon}\int_0^\tau \|F(Y^s f_1) - F(Y^s f_2)\|\,\mathrm{d}s\\ &\le \|f_1 - f_2\| + \frac{M}{\epsilon}\int_0^\tau \|Y^s f_1 - Y^s f_2\|\,\mathrm{d}s.\end{aligned}$$

An application of the Gronwall lemma leads to

$$\|Y^\tau f_1 - Y^\tau f_2\| \le \exp\left(\frac{M\tau}{\epsilon}\right)\|f_1 - f_2\|. \tag{4.2}$$

In particular, for $F(\psi) = \lambda|\psi|^2\psi$ we get

$$\|\mathcal{L}(\tau)f_1 - \mathcal{L}(\tau)f_2\| \le \exp\left(\frac{M\lambda\tau}{\epsilon}\right)\|f_1 - f_2\|. \tag{4.3}$$

Besides, for the nonlinear flow (4.1), we have the following lemma.

Lemma 4.2. *Let $\psi \in H^2$; if $F(\psi) = \lambda|\psi|^2\psi$, there exists a constant C such that for all $0 \le \tau \le 1$*

$$\|Y^\tau\psi\|_{H^2} \le \exp\left(\frac{\lambda\tau\|\psi\|_\infty^2}{\epsilon}\right)\|\psi\|_{H^2}. \tag{4.4}$$

If $F(\psi) = \lambda|\psi|^2\psi + v\psi$, there exists a constant C such that for $v \in H^2$ and for all $0 \le \tau \le 1$

$$\|Y^\tau\psi\|_{H^2} \le \exp\left(\frac{\tau\big(\|v\|_{H^2} + \lambda\|\psi\|_\infty^2\big)}{\epsilon}\right)\|\psi\|_{H^2}. \tag{4.5}$$

Proof. Consider $F(\psi) = \lambda|\psi|^2\psi + v\psi$. For the nonlinear flow (4.1), we have

$$\|Y^\tau\psi\|_\infty \le \|\psi\|_\infty + \frac{1}{\epsilon}\int_0^\tau \|F(Y^s\psi)\|_\infty\,\mathrm{d}s \le \|\psi\|_\infty + \frac{\|v\|_\infty + \lambda\|\psi\|_\infty^2}{\epsilon}\int_0^\tau \|Y^s\psi\|_\infty\,\mathrm{d}s.$$

Then the application of Gronwall inequality yields

$$\|Y^\tau\psi\|_\infty \le \exp\left(\frac{\tau\big(\|v\|_\infty + \lambda\|\psi\|_\infty^2\big)}{\epsilon}\right)\|\psi\|_\infty.$$

Similarly, for the H^2 norm, we directly have

$$\|Y^\tau\psi\|_{H^2} \le \|\psi\|_{H^2} + \frac{\|v\|_{H^2} + \lambda\|\psi\|_\infty^2}{\epsilon}\int_0^\tau \|Y^s\psi\|_{H^2}\,\mathrm{d}s,$$

which also leads to

$$\|Y^\tau\psi\|_{H^2} \le \exp\left(\frac{\tau\big(\|v\|_{H^2} + \lambda\|\psi\|_\infty^2\big)}{\epsilon}\right)\|\psi\|_{H^2}.$$

Let $v = 0$ and we get (4.4). This completes the proof. □

For the semi-discretized time-splitting methods, we have the following convergence theorem.

Theorem 4.1. *Let $\psi_{\text{in}} \in H^4$, $T > 0$ and $\Delta t \in (0, \epsilon)$. For $n\Delta t \le T$, there exists a constant C such that*

$$\left\|\mathcal{L}^n\psi_{\text{in}} - S^{n\Delta t}\psi_{\text{in}}\right\| \le CT\|\psi_{\text{in}}\|_{H^4}\left(1 + \frac{T}{\epsilon}\right)\frac{\Delta t^2}{\epsilon^3}. \tag{4.6}$$

Proof. Similar to the proof in [10,16]. Using the triangle inequality yields

$$\left\|\mathcal{L}^n\psi_{\text{in}} - S^{n\Delta t}\psi_{\text{in}}\right\| \le \sum_{j=0}^{n-1}\left\|\mathcal{L}^{n-j}S^{j\Delta t}\psi_{\text{in}} - \mathcal{L}^{n-j-1}S^{(j+1)\Delta t}\psi_{\text{in}}\right\|.$$

Due to S^t being the Lie formula for all $t \le T$ and $\psi_{\text{in}} \in H^4$, $S^t\psi_{\text{in}}$ belongs to H^4 and is uniformly bounded in this space, thus for all j such that $j\Delta t \le T$, we have

$$\left\|\mathcal{L}S^{j\Delta t}\psi_{\text{in}} - S^{(j+1)\Delta t}\psi_{\text{in}}\right\| = \left\|\left(\mathcal{L} - S^{\Delta t}\right)S^{j\Delta t}\psi_{\text{in}}\right\| \le C\|\psi_{\text{in}}\|_{H^4}\frac{\Delta t^3}{\epsilon^3}.$$

Combine with (4.3) and we get

$$\left\|\mathcal{L}^n\psi_{\text{in}} - S^{n\Delta t}\psi_{\text{in}}\right\| \le \sum_{j=0}^{n-1}\left(\exp\left(\frac{M\lambda\Delta t}{\epsilon}\right)\right)^{n-j-1}\left\|\left(\mathcal{L} - S^{\Delta t}\right)S^{j\Delta t}\psi_{\text{in}}\right\|.$$

Since $0 < \Delta t < \epsilon$, for all $j \ge 0$, we have

$$\left(\exp\left(\frac{M\lambda\Delta t}{\epsilon}\right)\right)^j \le \left(1 + C_0\frac{\Delta t}{\epsilon}\right)^j \le 1 + Cj\frac{\Delta t}{\epsilon}.$$

Consequently, we arrive at

$$\begin{aligned}\left\|\mathcal{L}^n\psi_{\text{in}} - S^{n\Delta t}\psi_{\text{in}}\right\| &\le \sum_{j=0}^{n-1}\left(\exp\left(\frac{M\lambda\Delta t}{\epsilon}\right)\right)^{n-j-1} C\|\psi_{\text{in}}\|_{H^4}\frac{\Delta t^3}{\epsilon^3}\\ &\le C\|\psi_{\text{in}}\|_{H^4}\frac{\Delta t^3}{\epsilon^3}\sum_{j=0}^{n-1}\left(1 + C(n-j-1)\frac{\Delta t}{\epsilon}\right) \le CT\|\psi_{\text{in}}\|_{H^4}\left(1 + \frac{T}{\epsilon}\right)\frac{\Delta t^2}{\epsilon^3}.\end{aligned}$$

It concludes the proof of this theorem. □

Next, we give the convergence of the full TS-FEM method. Consider the problem

$$i\epsilon\partial_t\psi^\epsilon = \mathcal{L}_2\psi^\epsilon$$

with the initial condition ψ_{in} and the periodical boundary condition. The solution has the form

$$\psi^\epsilon(\boldsymbol{x},t)=\exp\left(-\frac{it}{2\epsilon}\mathcal{L}_2\right)\psi_{\text{in}}(\boldsymbol{x}). \tag{4.7}$$

If $\mathcal{L}_2$ consists of potential and nonlinear term, the regularity of $\psi^\epsilon(t,\boldsymbol{x})$ depends on the regularity of both the potential v and ψ_{in}, otherwise it only depends on ψ_{in}.

Assume that the numerical solution ψ_h^ϵ solves (3.11) and $\psi^\epsilon(t_n)=S^{n\Delta t}\psi_{\text{in}}$ is the solution of (2.1). We write

$$\psi_h^{\epsilon,n}-\psi^\epsilon(t_n)=L^n\psi_h^0-S^{n\Delta t}\psi_{\text{in}}=\left(L^n\psi_h^0-\mathcal{L}^n\psi_{\text{in}}\right)+\left(\mathcal{L}^n\psi_{\text{in}}-S^{n\Delta t}\psi_{\text{in}}\right). \tag{4.8}$$

The first term denotes the error attributable to the space discretization and the second term is the time-splitting error.

We now estimate the spatial error accommodation from $t=0$ to $t=\Delta t$,

$$\psi_h^{\epsilon,1}-\psi^\epsilon(\Delta t)=L_2\left(\frac{\Delta t}{2},\cdot\right)\circ L_1(\Delta t)L_2\left(\frac{\Delta t}{2},\cdot\right)\circ\psi_h^0-\mathcal{L}(\Delta t)\psi_{\text{in}}.$$

Let $\hat{\psi}_0=\mathcal{L}_2(\frac{\Delta t}{2},\cdot)\circ\psi_{\text{in}}$, and consider the problem

$$i\epsilon\partial_t\psi^\epsilon=-\frac{\epsilon^2}{2}\Delta\psi^\epsilon+v\psi^\epsilon \tag{4.9}$$

with the initial condition $\psi^\epsilon(t=0)=\hat{\psi}_0$ and the periodical boundary condition. The corresponding weak form is

$$i\epsilon\left(\partial_t(\psi^\epsilon-\psi_h^\epsilon),\phi^h\right)=\frac{\epsilon^2}{2}\left(\nabla(\psi^\epsilon-\psi_h^\epsilon),\nabla\phi^h\right)+\left(v(\psi^\epsilon-\psi_h^\epsilon),\phi^h\right),\quad\forall\phi^h\in V_h. \tag{4.10}$$

Let $\psi^\epsilon-\psi_h^\epsilon=(\psi^\epsilon-R_h\psi^\epsilon)+\theta$, where $\theta=R_h\psi^\epsilon-\psi_h^\epsilon$ and $R_h\psi^\epsilon$ denotes the Ritz projection. According to (4.10), we get

$$i\epsilon\left(\partial_t[(\psi^\epsilon-R_h\psi^\epsilon)+\theta],\phi^h\right)=\frac{\epsilon^2}{2}\left(\nabla\theta,\nabla\phi^h\right)+\left(v(\psi^\epsilon-R_h\psi^\epsilon),\phi^h\right)+\left(v\theta,\phi^h\right). \tag{4.11}$$

Take $\phi^h=\theta$ in the above equation,

$$i\epsilon(\partial_t\theta,\theta)=-i\epsilon(\partial_t(\psi^\epsilon-R_h\psi^\epsilon),\theta)+\frac{\epsilon^2}{2}\|\nabla\theta\|^2+(v(\psi^\epsilon-R_h\psi^\epsilon),\theta)+(v\theta,\theta),$$

and we have

$$i\epsilon\,\mathrm{d}_t\|\theta\|^2=i\epsilon(\partial_t\theta,\theta)+i\epsilon\left(\partial_t\bar{\theta},\bar{\theta}\right)=2i\epsilon\Re(\partial_t(\psi^\epsilon-R_h\psi^\epsilon),\theta)+2i\Im(v(\psi^\epsilon-R_h\psi^\epsilon),\theta),$$

which induces

$$\mathrm{d}_t\|\theta\|\le 2\|\partial_t(\psi^\epsilon-R_h\psi^\epsilon)\|+\frac{2}{\epsilon}\|v\|_\infty\|\psi^\epsilon-R_h\psi^\epsilon\|. \tag{4.12}$$

Integrating from 0 to t yields

$$\|\theta(t)\|\le\|\theta(0)\|+2\int_0^t\|\partial_t(\psi^\epsilon-R_h\psi^\epsilon)\|\,\mathrm{d}t+\frac{2}{\epsilon}\|v\|_\infty\int_0^t\|\psi^\epsilon-R_h\psi^\epsilon\|\,\mathrm{d}t. \tag{4.13}$$

Assume $\|\theta(0)\|=\|\hat{\psi}_{\text{in}}-R_h\hat{\psi}_{\text{in}}\|=\|\psi_{\text{in}}-R_h\psi_{\text{in}}\|=0$. Since $\|R_h\partial_t\psi^\epsilon-\partial_t\psi^\epsilon\|\le Ch^2\|\partial_t\psi^\epsilon\|_{H^2}$, we have

$$\|\theta(t)\|\le Cth^2\|\partial_t\psi^\epsilon\|_{H^2}+\frac{Ch^2}{\epsilon}\int_0^t\|\psi^\epsilon\|_{H^2}\,\mathrm{d}s\le C_{\lambda,\epsilon}th^2+\frac{Cth^2}{\epsilon^3}\le CC_{\lambda,\epsilon}th^2, \tag{4.14}$$

where $t \le \Delta t$, and $C_{\lambda,\epsilon}$ is the leading order term with respect to ϵ^{-1}.

Let $\hat{\psi}_{h,1}$ be the numerical solution of (4.9) with $t = \Delta t$, and we obtain

$$\begin{aligned}\left\|\psi_h^{\epsilon,1} - \psi^\epsilon(\Delta t)\right\| &= \left\|\exp\left(-\frac{i\Delta t L_2\left(\hat{\psi}_{h,1}\right)}{2\epsilon}\right)\hat{\psi}_{h,1} - \exp\left(-\frac{i\Delta t \mathcal{L}_2\left(\hat{\psi}_1\right)}{2\epsilon}\right)\hat{\psi}_1\right\| \\ &\le \left\|\exp\left(-\frac{i\Delta t L_2\left(\hat{\psi}_{h,1}\right)}{2\epsilon}\right)\hat{\psi}_{h,1} - \exp\left(-\frac{i\Delta t L_2\left(\hat{\psi}_1\right)}{2\epsilon}\right)\hat{\psi}_1\right\| \\ &\quad + \left\|\exp\left(-\frac{i\Delta t L_2\left(\hat{\psi}_{h,1}\right)}{2\epsilon}\right)\hat{\psi}_1 - \exp\left(-\frac{i\Delta t \mathcal{L}_2\left(\hat{\psi}_1\right)}{2\epsilon}\right)\hat{\psi}_1\right\| \\ &\le C\exp\left(\frac{M\lambda\Delta t}{2\epsilon}\right)\|\theta(t)\|,\end{aligned}$$

in which we use the Lipschitz linearity of the nonlinear flow and $\hat{\psi}_1 = \exp(-\frac{i\epsilon\Delta t\mathcal{L}_1}{\epsilon})\exp(-\frac{i\epsilon\Delta t\mathcal{L}_2}{2\epsilon})\psi_{\text{in}}$. This indicates the spatial error accumulation in a one-time step. We next estimate the error accumulation in both time and space from $t = 0$ to T.

Theorem 4.2. *Assume that $\psi_h^{\epsilon,n} = L^n\psi_{\text{in}}$ and $\psi^\epsilon(n\Delta t) = S^{n\Delta t}\psi_{\text{in}}$ are the numerical solution and exact solution of the NLSE. Moreover, assume $\partial_t\psi^\epsilon \in H^2$ for all $t \in [0,T]$ and $\psi_{\text{in}} \in H^4$. Then for a given $T > 0$, there exists a constant h_0 such that $h \le h_0$ and for all $\Delta t < \epsilon$ with $n\Delta t \le T$, and the L^2 error estimate satisfies*

$$\|\psi_h^{\epsilon,n} - \psi^\epsilon(n\Delta t)\| \le CC_{\lambda,\epsilon}h^2 + CT\left(1 + \frac{T}{\epsilon}\right)\frac{\Delta t^2}{\epsilon^3}, \tag{4.15}$$

where the constant C is independent of ϵ and T.

Proof. The error can be split into

$$\psi_h^{\epsilon,n} - \psi^\epsilon(n\Delta t) = L^n\psi_h^0 - S^{n\Delta t}\psi_{\text{in}} = \left(L^n\psi_h^0 - \mathcal{L}^n\psi_{\text{in}}\right) + \left(\mathcal{L}^n\psi_{\text{in}} - S^{n\Delta t}\psi_{\text{in}}\right).$$

The first term on the right-hand side satisfies

$$\left\|L^n\psi_h^0 - \mathcal{L}^n\psi_{\text{in}}\right\| \le \left\|\sum_{j=1}^n L^{n-j}(LR_h - R_h\mathcal{L})\mathcal{L}^{j-1}\psi_{\text{in}}\right\| + \|(R_h - I)\mathcal{L}^n\psi_{\text{in}}\|.$$

Due to $\mathcal{L}_1$ conserving the H^2 norm of the solution and Lemma 4.2, we have $\mathcal{L}^n\psi_{\text{in}} \in H^2$ and $\|(R_h - I)\mathcal{L}^n\psi_{\text{in}}\| \le Ch^2\|\mathcal{L}^n\psi_{\text{in}}\|_{H^2}$. Meanwhile,

$$\|L\psi^\epsilon\| \le \|L\psi^\epsilon - \mathcal{L}(\Delta t)\psi^\epsilon\| + \|\mathcal{L}(\Delta t)\psi^\epsilon\| \le CC_{\lambda,\epsilon}\Delta t h^2 + \|\psi^\epsilon\|.$$

Similar to Theorem 3.1 in [4], we denote the bound of the numerical solution by

$$\max_{1\le m\le n}\left\|L^m R_h\mathcal{L}^{n-m}\psi^\epsilon\right\| \le a_L.$$

Recall (4.13) and (4.14), owing to $\Delta t < \epsilon$, then there exists a constant C independent of ϵ such that

$$\left\|\sum_{j=1}^n L^{n-j}(LR_h - R_h\mathcal{L})\mathcal{L}^{j-1}\psi_{\text{in}}\right\| \le n\exp\left(CTa_L^2\right)\max_{1\le j\le n}\left\|(LR_h - R_h\mathcal{L})\mathcal{L}^{j-1}\psi_{\text{in}}\right\|$$

$$\leq n\exp\left(CTa_L^2\right)\exp\left(\frac{\lambda M\Delta t}{\epsilon}\right)CC_{\lambda,\epsilon}\Delta t h^2 \leq \exp\left(CTa_L^2\right)\exp\left(\frac{\lambda M\Delta t}{\epsilon}\right)CC_{\lambda,\epsilon}Th^2.$$

Thus, we arrive at

$$\|L^n\psi_{\text{in}} - \mathcal{L}^n\psi_{\text{in}}\| \leq CC_{\lambda,\epsilon}h^2,$$

where C is independent of ϵ but depends on T and λ. Note that the order of $\|\psi^\epsilon\|_{H^2}$ with respect to ϵ^{-1} is lower than $C_{\lambda,\epsilon}$, and it is ignored in this result.

Furthermore, combine with Theorem 4.1, and we get the desired estimate

$$\begin{aligned}\|\psi_h^{\epsilon,n} - \psi^\epsilon(n\Delta t)\| &\leq \|L^n\psi_{\text{in}} - \mathcal{L}^n\psi_{\text{in}}\| + \left\|\mathcal{L}^n\psi_{\text{in}} - S^{n\Delta t}\psi_{\text{in}}\right\| \\ &\leq CC_{\lambda,\epsilon}h^2 + CT\left(1+\frac{T}{\epsilon}\right)\frac{\Delta t^2}{\epsilon^3}.\end{aligned}$$

This declares the (4.15). □

Remark 4.1. Take a further simplification

$$\frac{C}{\epsilon^3}\left(1+\frac{T}{\epsilon}\right) \leq \frac{CT}{\epsilon^4}.$$

We temporarily use $\psi_H^{\epsilon,n}$ to denote the FEM solution on the coarse mesh with mesh size H, the counterpart result of Theorem 4.2 on the coarse space is

$$\|\psi_H^{\epsilon,n} - \psi^\epsilon(n\Delta t)\| \leq CC_{\lambda,\epsilon}H^2 + \frac{CT^2}{\epsilon^4}\Delta t^2. \tag{4.16}$$

We have obtained the L^2 error estimate of the TS-FEM applied to the deterministic NLSE. Next, we will further assess the convergence analysis of the multiscale method, in conjunction with the qMC method. Note that the convergence analysis for the TS-FEM combined with the qMC method follows a similar pattern. Therefore, we will not discuss the convergence analysis of the TS-FEM in random space in this section.

4.2. Convergence analysis of the time-splitting multiscale method for NLSE with random potentials

4.2.1. The time-splitting multiscale method for the deterministic NLSE

For **SI**, we solve the linear Schrödinger equation by the multiscale method and the corresponding convergence analysis has been given in [59]. We therefore have the following estimate.

Lemma 4.3. *Let $\psi_H^{\epsilon,n} = L_{ms}^n\psi_{\text{in}}$ be the numerical solution solved in V_{ms} by* **SI**, *and $\psi^\epsilon(t_n) = S^{n\Delta t}\psi_{\text{in}}$ be the exact solution of the NLSE. Let $\Delta t \in (0,\epsilon)$, and assume $\partial_t\psi^\epsilon \in L^2$ for all $t \in (0,T]$, and $\psi_{\text{in}} \in H^4$. We have the estimate*

$$\|\psi_H^{\epsilon,n} - \psi^\epsilon(t_n)\| \leq \frac{CTH^2}{\epsilon^3} + \frac{CT^2}{\epsilon^4}\Delta t^2, \tag{4.17}$$

where the constant C is independent of ϵ.

Proof. For the linear Schrödinger equation, the spatial error of multiscale solution and exact solution has the bound [59]

$$\|\psi_H^\epsilon - \psi^\epsilon\| \leq \frac{CH^2}{\epsilon^2}\|\epsilon\partial_t\psi^\epsilon\| \leq \frac{CH^2}{\epsilon}\|\partial_t\psi_{\text{in}}\|\exp\left(\frac{2\lambda t\|\psi^\epsilon\|_\infty^2}{\epsilon}\right).$$

At the second step of **SI**, we have

$$\|\psi_H^\epsilon - \psi^\epsilon\| \le \frac{CH^2}{\epsilon^2} \exp\left(\frac{2\lambda\Delta t\|\psi^\epsilon\|_\infty^2}{\epsilon}\right) \le \frac{CH^2}{\epsilon^2}.$$

When the eigendecomposition method is applied, the solution can be solved exactly in time for linear problems. The accumulation of the spatial error at each time step satisfies

$$\begin{aligned}\|L_{ms}\psi_H^{\epsilon,n} - \mathcal{L}\psi^{\epsilon,n}\| &\le \|L_{ms}\psi_H^{\epsilon,n} - \mathcal{L}I_H\psi^{\epsilon,n}\| + \|\mathcal{L}I_H\psi^{\epsilon,n} - \mathcal{L}\psi^{\epsilon,n}\| \\ &\le \exp\left(\frac{\lambda M\Delta t}{2\epsilon}\right)\frac{CH^2}{\epsilon^2} + \exp\left(\frac{\lambda M\Delta t}{\epsilon}\right)\|I_H\psi^{\epsilon,n} - \psi^{\epsilon,n}\| \le \exp\left(\frac{\lambda M\Delta t}{\epsilon}\right)\frac{CH^2}{\epsilon^2}.\end{aligned}$$

Meanwhile, by the Strang splitting method, repeat the procedures in Theorem 4.1, and we get the estimate as (4.17). □

Remark 4.2. In comparison to Remark 4.1, the multiscale method exhibits superior performance with respect to ϵ, as it requires only the bound $\|\partial_t\psi^\epsilon\|$. In contrast, the application of the classical FEM requires the bound of $\|\partial_t\psi^\epsilon\|_{H^2}$, which implies a stronger dependence on ϵ. Consequently, the weaker dependence of multiscale method on ϵ demonstrates its superiority in effectively handling multiscale problems.

4.2.2. The multiscale method for the NLSE with random potentials

To carry out the convergence analysis for the qMC method, the regularity of the wave function with respect to random variables is required. The random potential is truncated by the m-order KL expansion, and we denote $\boldsymbol{\xi}(\omega) = (\xi_1(\omega), \cdots, \xi_m(\omega))^T$. Let $\boldsymbol{\nu} = (\nu_1, \cdots, \nu_m)$ be the multi-index with ν_j being the nonnegative integer, where $|\boldsymbol{\nu}| = \sum_{j=1}^m \nu_j$. Then $\partial^{\boldsymbol{\nu}}\psi_m^\epsilon$ denotes the mixed derivative of ψ_m^ϵ with respect to all random variables specified by the multi-index $\boldsymbol{\nu}$.

Lemma 4.4. *For any $\omega \in \Omega$ and multi-index $|\boldsymbol{\nu}| < \infty$, and for all $t \in (0, T]$, there exists a constant $C(T, \lambda, \epsilon, |\boldsymbol{\nu}|)$ depends on $T, \lambda, \epsilon, |\boldsymbol{\nu}|$ such that the partial derivative of $\psi_m^\epsilon(t, \boldsymbol{x}, \omega)$ satisfies a priori estimate*

$$\|\partial^{\boldsymbol{\nu}}\psi_m\|_{H^2} \le C(T, \lambda, \epsilon, |\boldsymbol{\nu}|)\prod_j\left(\sqrt{\lambda_j}\|v_j\|_{H^2}\right)^{\nu_j}. \tag{4.18}$$

The proof of this lemma is given in the appendix.

We are interested in the expectation of linear functionals of the numerical solution in applications of uncertainty quantification. We will estimate the expected value $\mathbb{E}[\mathcal{G}(\psi_m^\epsilon(\cdot, \omega))]$ of the random variable $\mathcal{G}(\psi_m^\epsilon(\cdot, \omega))$. Let $\mathcal{G}(\cdot)$ be a continuous linear functional on $L^2(\mathcal{D})$, then there exists a constant $C_\mathcal{G}$ such that

$$|\mathcal{G}(u)| \le C_\mathcal{G}\|u\|$$

for all $u \in L^2(\mathcal{D})$. Consider the integral

$$I_m(F) = \int_{\boldsymbol{\xi}\in[0,1]^m} F(\boldsymbol{\xi})\,\mathrm{d}\boldsymbol{\xi}, \tag{4.19}$$

where $F(\boldsymbol{\xi}) = \mathcal{G}(\psi_m^\epsilon(\cdot, \boldsymbol{\xi}))$. To approximate this integral, both the MC and qMC can be used. In our methods, it is approximated over the unit cube by randomly shifted lattice rules

$$Q_{m,n}(\boldsymbol{\Delta}; F) = \frac{1}{N}\sum_{i=1}^N F\left(\mathrm{frac}\left(\frac{iz}{N} + \boldsymbol{\Delta}\right)\right),$$

where $z \in \mathbb{N}^m$ is the generating vector, $\boldsymbol{\Delta} \in [0, 1]^m$ and "frac" is the fractional part function applying componentwise. Here N denotes the number of random samples.

Lemma 4.5. *For the integral (4.19), given $m, N \in \mathbb{N}$ with $N \leq 10^{30}$, weights $\gamma = (\gamma_{\mathbf{u}})_{\mathbf{u}\subset\mathbb{N}}$, a randomly shifted lattice rule with N points in m dimensional random space could be constructed by a component-by-component such that for all $\alpha \in (\frac{1}{2}, 1]$*

$$\sqrt{\mathbb{E}^{\boldsymbol{\Delta}}|I_m(F) - Q_{m,N}(\cdot; F)|} \leq 9C^* C_{\gamma,m}(\alpha) N^{-1/2\alpha},$$

where

$$C_{\gamma,m}(\alpha) = \left(\sum_{\emptyset\neq\mathbf{u}\subseteq\{1:m\}} \gamma_{\mathbf{u}}^{\alpha} \prod_{j\in\mathbf{u}} \varrho(\alpha)\right)^{1/2\alpha} \left(\sum_{\mathbf{u}\subseteq\{1:m\}} \frac{(C(\boldsymbol{\nu}))^2}{\gamma_{\mathbf{u}}} \prod_{j\in\mathbf{u}} \lambda_j \|v_j\|_{H^2}^2\right)^{1/2}.$$

Proof. The proof of the lemma is the same as in [14]. Here $C(\boldsymbol{\nu}) = C(t, \lambda, \epsilon, |\boldsymbol{\nu}|)$ is calculated in Lemma 4.4. And

$$\varrho(\alpha) = 2\left(\frac{\sqrt{2\pi}}{\pi^{2-2\eta_*(1-\eta_*)\eta_*}}\right)^{\alpha} \zeta\left(\alpha + \frac{1}{2}\right), \tag{4.20}$$

where $\eta_* = \frac{2\alpha-1}{4\alpha}$, $\zeta(x)$ is the Riemann zeta function and $C^* = \|\mathcal{G}\|$. The details of these estimates can be found in [17, 25]. □

Employing the qMC method, the estimate between the wave functions of (2.1) and the truncated NLSE (2.10) satisfies the following lemma.

Lemma 4.6. *Under the Assumption 2.2, there exists a constant C such that*

$$\sqrt{\mathbb{E}^{\boldsymbol{\Delta}}\left[|\mathbb{E}[\mathcal{G}(\psi^\epsilon)] - Q_{m,N}[\mathcal{G}(\psi_m^\epsilon)]|^2\right]} \leq C\left(\frac{m^{-\chi}}{\epsilon} + C_{\gamma,m} N^{-r}\right), \tag{4.21}$$

where $0 \leq \chi \leq (\frac{1}{2} - \eta)\Theta - \frac{1}{2}$, $r = 1 - \delta$ for $0 < \delta < \frac{1}{2}$. Note that the constant C is independent of m and n but depends on T.

Proof. Since $\mathcal{G}$ is a linear functional, we have

$$\begin{aligned}|\mathbb{E}[\mathcal{G}(\psi^\epsilon)] - Q_{m,N}[\mathcal{G}(\psi_m^\epsilon)]| &\leq |\mathbb{E}[\mathcal{G}(\psi^\epsilon)] - I_m(\psi^\epsilon)| + |I_m(\psi^\epsilon) - Q_{m,N}[\mathcal{G}(\psi_m^\epsilon)]| \\ &= |\mathbb{E}[\mathcal{G}(\psi^\epsilon)] - \mathbb{E}[\mathcal{G}(\psi_m^\epsilon)]| + |I_m(\psi^\epsilon) - Q_{m,N}[\mathcal{G}(\psi_m^\epsilon)]|.\end{aligned}$$

The first term satisfies

$$|\mathbb{E}[\mathcal{G}(\psi^\epsilon)] - \mathbb{E}[\mathcal{G}(\psi_m^\epsilon)]| \leq \mathbb{E}[|\mathcal{G}(\psi^\epsilon) - \mathcal{G}(\psi_m^\epsilon)|] \leq C\frac{m^{-\chi}}{\epsilon},$$

where C depends on the time T. Let $\alpha = 1/(2-2\delta)$ for $0 < \delta < \frac{1}{2}$, according to Lemma 4.5, we then get

$$\begin{aligned}&\mathbb{E}^{\boldsymbol{\Delta}}\left[|\mathbb{E}[\mathcal{G}(\psi^\epsilon)] - Q_{m,N}[\mathcal{G}(\psi_m^\epsilon)]|^2\right] \\ \leq&\mathbb{E}^{\boldsymbol{\Delta}}[|\mathbb{E}[\mathcal{G}(\psi^\epsilon)] - I_m(\psi^\epsilon)|^2] + \mathbb{E}^{\boldsymbol{\Delta}}[|I_m(\psi^\epsilon) - Q_{m,N}[\mathcal{G}(\psi_m^\epsilon)]|^2] \\ \leq&C\frac{m^{-2\chi}}{\epsilon^2} + CC_{\gamma,m}^2 N^{2-2\delta}.\end{aligned}$$

□

Employ the qMC method in the random space, for the numerical solution $\psi_H^{\epsilon,m}$ solved by the multiscale method, and we have the following error estimate.

Theorem 4.3. *Let $\psi_{\text{in}} \in H^4(\mathcal{D})$, $\psi^\epsilon \in L^\infty([0,T];H^4(\mathcal{D})) \cap L^1([0,T];H^2(\mathcal{D}))$, and parameterized potentials satisfy the Assumption 2.2. Consider $\mathbb{E}[\mathcal{G}(\psi^\epsilon(t_n))]$ is approximated by $Q_{m,N}(\cdot;\mathcal{G}(\psi^{\epsilon,n}_{H,m}))$. Apply the random shifted lattice rule $Q_{m,N}$ to $\mathcal{G}(\psi^\epsilon(t_n))$. Then for any fixed $T>0$, there exists a constant H_0 such that $H \le H_0$ and for all $\Delta t < \epsilon$ with $n\Delta t \le T$, we have the root-mean-square error as*

$$\sqrt{\mathbb{E}^{\boldsymbol{\Delta}}\left[\left|\mathbb{E}[\mathcal{G}(\psi^\epsilon(t_n))] - Q_{m,N}\left[\mathcal{G}\left(\psi^{\epsilon,n}_{H,m}\right)\right]\right|^2\right]} \le C\left(\frac{H^2}{\epsilon^3} + \frac{\Delta t^2}{\epsilon^4} + \frac{m^{-\chi}}{\epsilon} + C_{\gamma,m}N^{-r}\right), \tag{4.22}$$

where $0 \le \chi \le (\frac{1}{2}-\eta)\Theta - \frac{1}{2}$, and $r = 1-\delta$ for $0<\delta<\frac{1}{2}$. Here C is independent of m and N but depends on λ and T, and $C_{\gamma,m}$ depends on T, λ and ϵ.

Proof. We split the error (4.22) into

$$\begin{aligned}\left|\mathbb{E}[\mathcal{G}(\psi^\epsilon(t_n))] - Q_{m,N}\left[\mathcal{G}\left(\psi^{\epsilon,n}_{H,m}\right)\right]\right| &\le \left|\mathbb{E}[\mathcal{G}(\psi^\epsilon(t_n))] - Q_{m,N}[\mathcal{G}(\psi^\epsilon_m(t_n))]\right| \\ &\quad + \left|Q_{m,N}[\mathcal{G}(\psi^\epsilon_m(t_n))] - Q_{m,N}\left[\mathcal{G}\left(\psi^{\epsilon,n}_{H,m}\right)\right]\right|.\end{aligned}$$

The second term can be estimated by

$$\left|\mathcal{G}(\psi^\epsilon_m(t_n)) - \mathcal{G}\left(\psi^{\epsilon,n}_{H,m}\right)\right| \le C_{\mathcal{G}}\left\|\psi^\epsilon_m(t_n) - \psi^{\epsilon,n}_{H,m}\right\| \le CC_{\mathcal{G}}\left(\frac{H^2}{\epsilon^3} + \frac{\Delta t^2}{\epsilon^4}\right),$$

where the constant C depends on λ and T, and is independent of m and N. Combine with Lemma 4.6, we get the (4.22). This completes the proof. □

Remark 4.3. Theorem 4.3 gives the L^2 estimate of time-splitting multiscale method for the NLSE with random potentials. For the employment of the TS-FEM, repeat the above procedures and we can get a similar result.

5. Numerical experiments

In this part, we will present numerical experiments in both 1D and 2D physical space. The convergence rates of TS-FEM and TS-MM (time-splitting multiscale method) are first verified. For the NLSE with the random potential, we compare the convergence rate in the random space. In addition, the delocalization of mass distribution due to disordered potentials and the cubic nonlinearity is investigated.

5.1. Numerical accuracy of TS-FEMs

Set $\psi_{\text{in}}(x) = (10\pi)^{0.25}\exp(-20x^2)$ for the 1D case, and $\psi_{\text{in}}(x_1,x_2) = (10/\pi)^{0.25}\exp(-5(x_1-0.5)^2 - 5(x_2-0.5)^2)$ for the 2D case. To begin with, we choose the harmonic potential $v(x) = 0.5x^2$, and verify the second-order accuracy of the TS-FEM with respect to the temporal step size Δt and spatial mesh size h. Here we fix the terminal time $T = 1.0$, $\epsilon = \frac{1}{16}$ and nonlinear parameter $\lambda = 0.1$. The reference solution $\psi^\epsilon_{\text{ref}}$ is computed on the fine mesh with $h = \frac{2\pi}{2048}$ and $\Delta t = 1.0\text{e}{-}06$. The L^2 absolute error and H^1 absolute error are recorded in Table 1.

For the 2D case, we employ the multiscale potential

$$v(x_1,x_2) = \cos\left(x_1x_2 + \frac{x_1}{\epsilon} + \frac{x_1x_2}{\epsilon^2}\right), \tag{5.1}$$

over $\mathcal{D} = [0,1]^2$ with 64×64 spatial nodes. Here we set $\lambda = 1.0$ and multiscale coefficient $\epsilon = \frac{1}{8}$. We compare the numerical solution with the different Δt for **SI** and **SII**. By the means of the numerical tests shown in Figure 1, **SI** allows a bigger time step size than **SII**.

TABLE 1. Numerical convergence of TS-FEMs in space and time.

	h	$\frac{2\pi}{128}$	$\frac{2\pi}{256}$	$\frac{2\pi}{512}$	$\frac{2\pi}{1024}$	Order
SI	L^2 error	1.96e−02	5.22e−03	1.26e−03	2.54e−04	2.09
	H^1 error	1.19e−01	3.36e−02	8.31e−03	1.68e−03	2.04
SII	L^2 error	3.04e−02	8.07e−03	1.95e−03	3.92e−04	2.09
	H^1 error	3.52e−01	9.95e−02	2.44e−02	4.92e−03	2.05
	Δt	4.0e−02	2.0e−02	1.0e−02	5.0e−03	Order
SI	L^2 error	4.53e−04	1.13e−04	2.81e−05	7.03e−06	2.00
	H^1 error	2.09e−03	5.20e−04	1.30e−04	3.24e−05	2.00
SII	L^2 error	7.16e−03	1.87e−03	4.71e−04	1.18e−04	1.98
	H^1 error	1.12e−01	2.91e−02	7.26e−03	1.81e−03	1.99

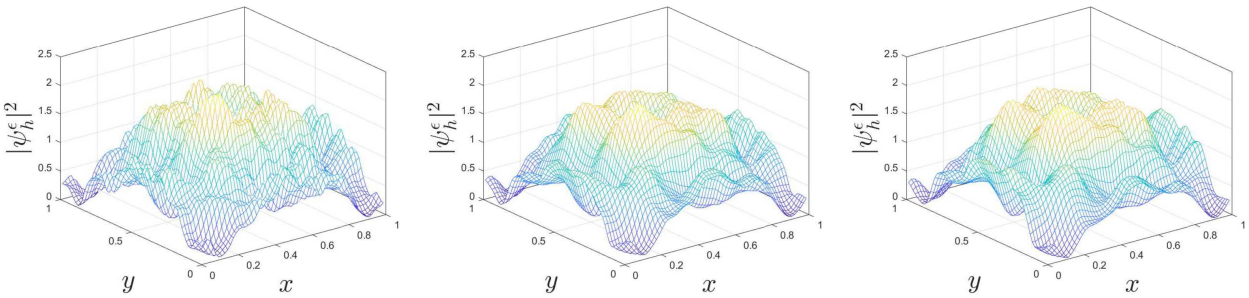

(A) (B) (C)

FIGURE 1. Numerical solution computed by the two TS-FEMs with different Δt. (a) **SI**, $\Delta t =$ 1.0e−2. (b) **SI**, $\Delta t =$ 1.0e−3. (c) **SII**, $\Delta t =$ 1.0e−3.

5.2. Numerical experiments of TS-MMs

In this study, we consider two forms of the multiscale solution: ψ_H^ϵ on the coarse mesh and $\psi_{H,h}^\epsilon$ on the fine mesh. We begin by employing the harmonic potential and varying the values of H. We then record the error between the numerical solution and the reference solution in Table 2. The simulation parameters used are: $\lambda = 0.1$, $\epsilon = \frac{1}{16}$, $T = 1.0$, $\Delta t =$1.0e−03, and a fine mesh size of $h = \frac{2\pi}{4096}$. Our results show that **SI** achieves a second-order convergence rate in both the coarse and fine spaces. Additionally, superconvergence is exhibited in the coarse space for **SII**.

Meanwhile, to demonstrate the advantages of Option 1, we examine the example of a discontinuous potential, as shown in Figure 2. We observe that **SI** maintains its second-order spatial convergence rate, whereas the convergence rate of **SII** deteriorates.

Furthermore, we consider the small semiclassical constant $\epsilon = \frac{1}{128}$ and the discontinuous potential as in Figure 2a. As shown in Figure 3, better approximations are provided by the multiscale method in the physical space.

For the 2D case, we consider the discontinuous checkboard potential

$$v_2 = \begin{cases} \left(\cos\left(2\pi\frac{x_1}{\epsilon_2}\right)+1\right)\left(\cos\left(2\pi\frac{x_2}{\epsilon_2}\right)+1\right), & [0,0.5]^2 \cup [0.5,1]^2, \\ \left(\cos\left(2\pi\frac{x_1}{\epsilon_1}\right)+1\right)\left(\cos\left(2\pi\frac{x_2}{\epsilon_1}\right)+1\right), & \text{otherwise}, \end{cases}$$

TABLE 2. Numerical convergence rate of the TS-MMs for the NLSE with harmonic potential in space.

	H	$\|\psi^\epsilon_{H,h} - \psi^\epsilon_{\text{ref}}\|$	$\|\psi^\epsilon_{H,h} - \psi^\epsilon_{\text{ref}}\|_{H^1}$	$\|\psi^\epsilon_{H} - \psi^\epsilon_{\text{ref}}\|$	$\|\psi^\epsilon_{H} - \psi^\epsilon_{\text{ref}}\|_{H^1}$
SI	$\frac{2\pi}{2048}$	4.95e−05	4.69e−04	3.47e−05	3.31e−04
	$\frac{2\pi}{1024}$	1.68e−04	1.60e−03	1.18e−04	1.13e−03
	$\frac{2\pi}{512}$	6.44e−04	6.11e−03	4.52e−04	4.32e−03
	$\frac{2\pi}{256}$	2.56e−03	2.43e−02	1.80e−03	1.72e−02
	Order	1.90	1.90	1.90	1.90
SII	$\frac{2\pi}{2048}$	1.79e−05	1.73e−04	5.43e−12	1.88e−10
	$\frac{2\pi}{1024}$	6.10e−05	5.86e−04	7.85e−11	1.63e−09
	$\frac{2\pi}{512}$	2.33e−04	2.24e−03	5.68e−09	1.02e−07
	$\frac{2\pi}{256}$	9.24e−04	8.89e−03	4.49e−07	8.24e−06
	Order	1.90	1.90	5.52	5.22

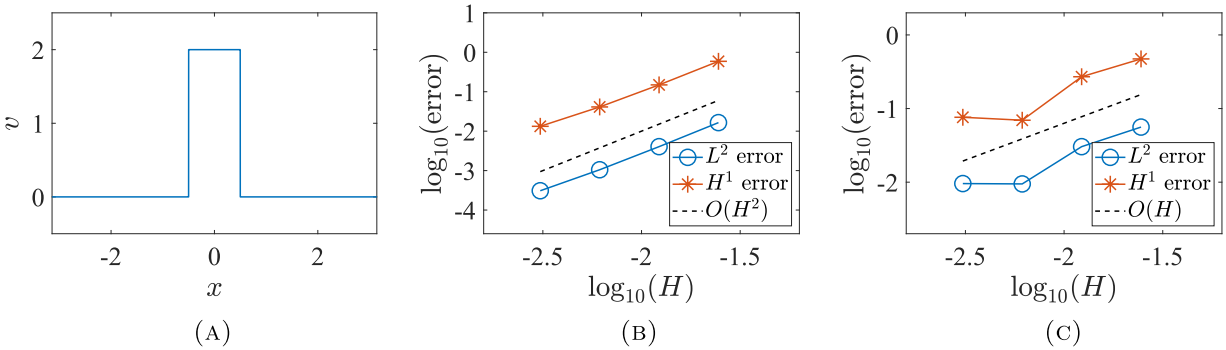

(A) (B) (C)

FIGURE 2. Numerical convergence rate of **SI** and **SII** for the discontinuous potential. In the plots, the L^2 error and H^1 error on the coarse mesh are depicted. (a) $v(\boldsymbol{x})$. (b) **SI**. (c) **SII**.

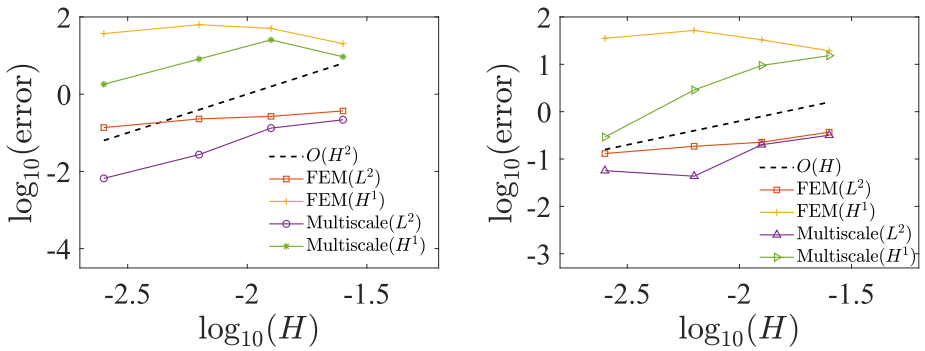

(A) (B)

FIGURE 3. The convergence rates of the FEM and the multiscale method for the NLSE with the discontinuous potential and semiclassical constant $\epsilon = \frac{1}{128}$. (a) **SI**. (b) **SII**.

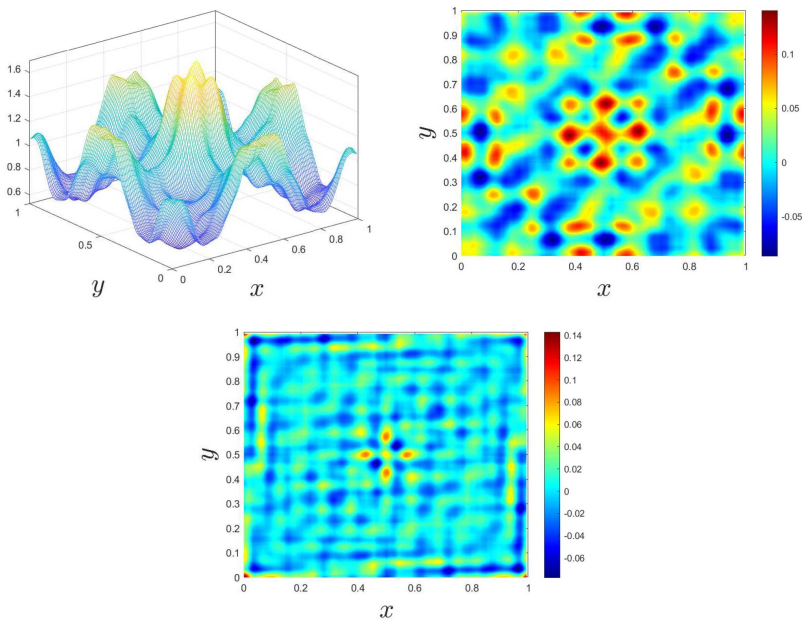

FIGURE 4. Reference solution (FEM) and the spatial error distribution computed by **SI**, in which the multiscale method is used with $H = 8h$ and $H = 4h$.

where $v = v_1 + v_2$ with $v_1 = |x_1 - 0.5|^2 + |x_2 - 0.5|^2$, $\epsilon_1 = \frac{1}{8}$ and $\epsilon_2 = \frac{1}{6}$. In the simulations, we set $h = \frac{1}{128}$, $\epsilon = \frac{1}{4}$, $\lambda = 1.0$, Δt =1.0e−04 and $T = 1.0$. We employ **SI** (Fig. 4) and **SII** (Fig. 5) for time evolution. We vary the coarse mesh size with $H = 4h$ and $H = 8h$ of the multiscale method and present the corresponding spatial error distribution. Here, the reference solution is obtained using the FEM with a mesh size of h. In both Figures 4 and 5, we observe a significant error when the multiscale method is used with a mesh size ratio of $H = 8h$. With the mesh being refined, the smaller error distribution in space can be obtained for **SI**. Hence this simulation demonstrates the superior performance of **SI** when dealing with discontinuous potentials.

5.3. Numerical simulations of NLSE with random potentials

For the 1D case, we consider the random potential

$$v(x,\omega) = \sigma \sum_{j=1}^{m} \sin(jx)\frac{1}{j^{\beta}}\xi_j(\omega), \tag{5.2}$$

where σ controls the strength of randomness, and $\xi_j(\omega)$'s are mean-zero and i.i.d random variables uniformly distributed in $[-\sqrt{3}, \sqrt{3}]$. It is extended to 2D as

$$v(x_1,x_2,\omega) = \sigma \sum_{j=1}^{m} \sin(jx_1)\sin(jx_2)\frac{1}{j^{\beta}}\xi_j(\omega). \tag{5.3}$$

For comparison, we employ the MC method and qMC method to generate the samples $\xi_j(\omega)$ in the simulations. And we measure the states of the system by the expectation of mass density

$$\mathbb{E}\left(\left|\psi^{\epsilon}_{H,h}\right|^2\right) = \frac{1}{N}\sum_{i}\left|\psi^{\epsilon}_{H,h}(\omega_i)\right|^2,$$

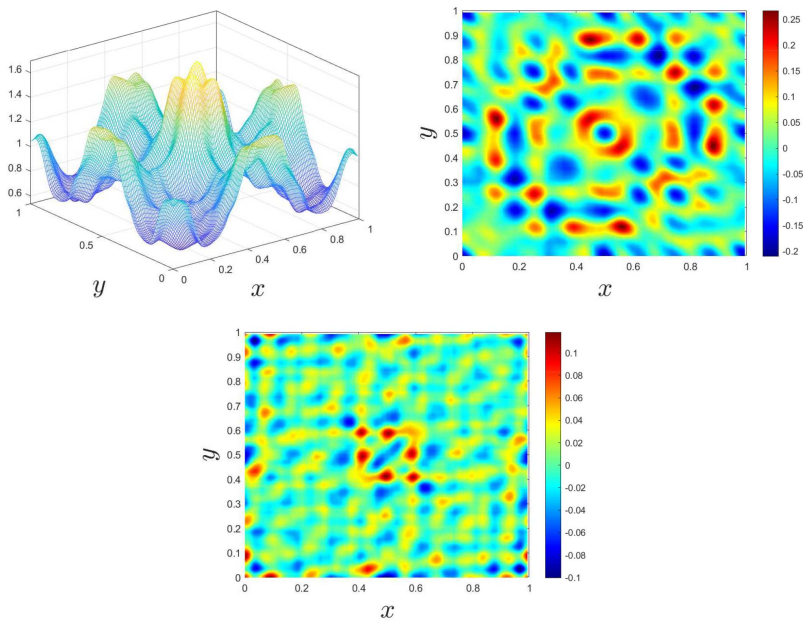

FIGURE 5. Reference solution (FEM) and the spatial error distribution computed by **SII**, in which the multiscale method is used with $H = 8h$ and $H = 4h$.

where N denotes the number of MC or qMC samples. To observe the evolution in the mass distribution of the system, we introduce the definition

$$A(t) = \mathbb{E}\left(\int_{\mathcal{D}} |\boldsymbol{x}|^2 |\psi^\epsilon|^2 \, \mathrm{d}\boldsymbol{x}\right), \tag{5.4}$$

which is extensively used to indicate the Anderson localization of the Schrödinger equation with random potentials.

5.3.1. Convergence of MC sampling and qMC sampling

The MC method and qMC method exhibit different convergence rates. To eliminate the perturbation of a small sample size, we adopt the random potential

$$v(x, \omega) = 1.0 + \sigma \sum_{j=1}^{m} \sin(jx) \frac{1}{j^\beta} \xi_j(\omega), \tag{5.5}$$

in which the parameters are: $\sigma = 1.0$, $\beta = 2.0$, $m = 5$. The other simulation settings are: $\lambda = 0.1$, $\epsilon = \frac{1}{8}$, $\mathcal{D} = [-\pi, \pi]$, $h = \frac{2\pi}{600}$, $H = 6h$, $T = 1.0$ and Δt =1.0e−03. In this experiment, we use 50 000 samples to compute the reference solution and record the L^2 error of the density $\|\mathbb{E}(|\psi^\epsilon_{\text{num}}|^2) - \mathbb{E}(|\psi^\epsilon_{\text{ref}}|^2)\|$ as the sampling number varies with $N = 100$, 200, 400, 800, 1600 and 3200 for both MC method and qMC method. The result is shown in Figure 6.

5.3.2. Investigation of wave propagation

To observe the wave propagation phenomena, we vary the nonlinear coefficient λ and record the evolution of $A(t)$. In addition, we depict $\mathbb{E}(|\psi^\epsilon_{H,h}|^2)$ at the final time. In these simulations, we generate 500 qMC samples to approximate the random potential. The parameters of simulations are: $\mathcal{D} = [-2\pi, 2\pi]$, $\sigma = 1.0$, $\beta = 0.0$, and $m = 5$. For the multiscale method, we fix $h = \frac{4\pi}{6000}$ and $H = 10h$. To observe the long-time behavior, we set the

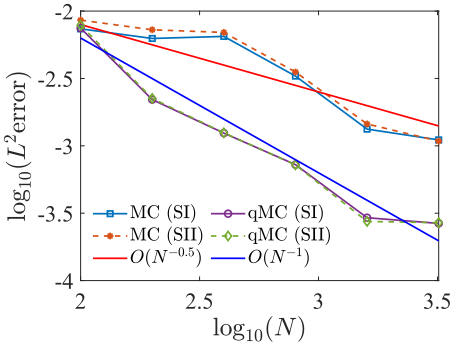

FIGURE 6. Numerical convergence rates of the MC and qMC methods.

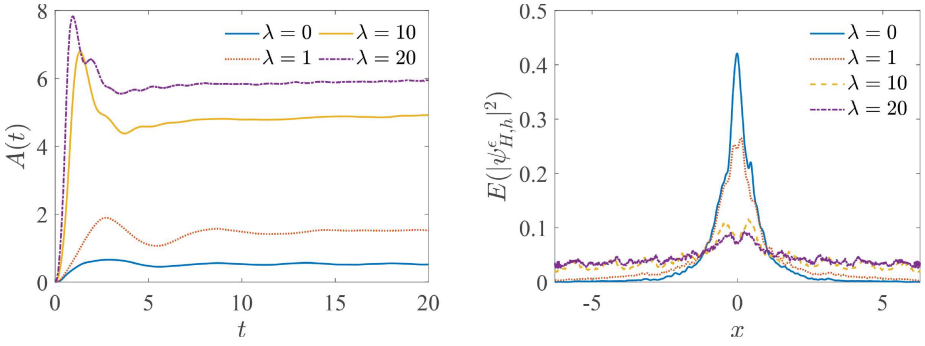

FIGURE 7. The evolution of $A(t)$ and density of expectation at $T = 20$, as the nonlinear coefficient λ varies. Results computed by the **SI** and the multiscale method.

terminal time to $T = 20$. We vary λ as 0, 1, 10, and 20, and the corresponding results are shown in Figure 7. One can see that $A(t)$ increases as time evolves for the nonlinear cases, while for the linear case, it remains within the range of $(0.51, 0.57)$ during the time interval from $t = 10$ to $t = 20$.

In the 2D case, we use the following settings in our numerical simulations: $h = \frac{1}{64}$, $\epsilon = \frac{1}{4}$, $H = 4h$, $\beta = 0$, $m = 5$, and $\sigma = 5$. Our results, depicted in Figures 8 and 9, show that while the localization of mass distribution is observed for the linear case, the nonlinear case exhibits delocalization.

6. Conclusion

In this paper, we have introduced two time-splitting finite element methods (TS-FEMs) for the cubic nonlinear Schrödinger equation (NLSE), incorporating a multiscale method to reduce spatial degrees of freedom. We have refined the optimization problems to eliminate the mesh dependence of multiscale basis functions introduced by local orthogonal normalization constraints. For the temporal evolution, we employed two Strang time-splitting techniques in which one maintains the convergence rate of the NLSE with discontinuous potentials. Meanwhile, we utilized the quasi-Monte Carlo sampling method to generate random potentials. Hence the proposed methods have second-order accuracy in both time and space and nearly first-order convergence in the random space. Furthermore, we provided a convergence analysis for the L^2 error estimate, which was verified through numerical experiments. Additionally, we presented a multiscale reduced basis method to alleviate the computational burden of constructing multiscale basis functions for random potentials. Using these methods, we investigated the long-

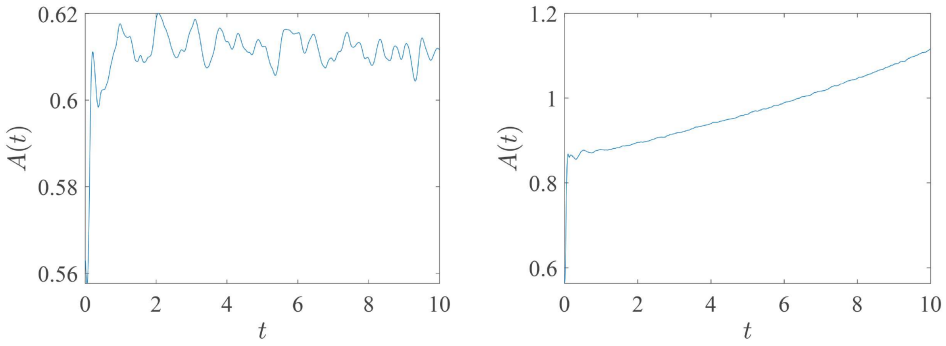

FIGURE 8. The evolution of $A(t)$ for 2D linear case and nonlinear case with $\lambda = 20$. Results are computed by **SI** and the multiscale method.

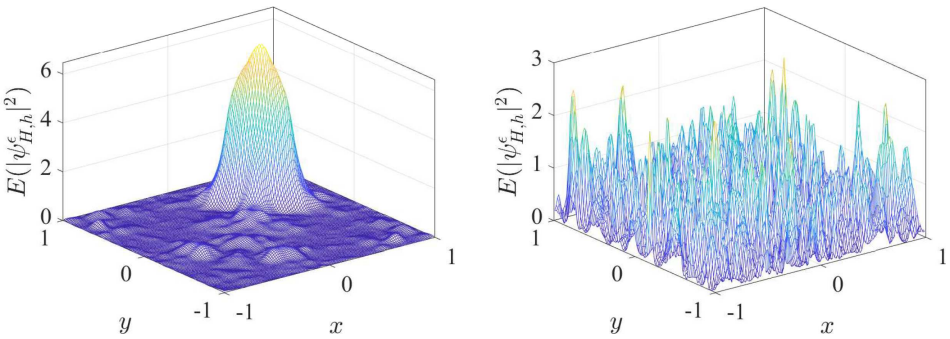

FIGURE 9. The localization and delocalization of mass distribution of the 2D linear Schrödinger equation and NLSE with random potentials, respectively.

term wave propagation of the NLSE with parameterized random potentials in 1D and 2D physical spaces, observing localization in the linear case and delocalization in the nonlinear case.

FUNDING

The research of Z. Zhang is supported by the National Natural Science Foundation of China (Projects 92470103 and 12171406), the Hong Kong RGC grant (Projects 17307921, 17304324, and 17300325), the Outstanding Young Researcher Award of HKU (2020–21), Seed Funding for Strategic Interdisciplinary Research Scheme 2021/22 (HKU), and seed funding from the HKU-TCL Joint Research Center for Artificial Intelligence. The computations were performed at the research computing facilities provided by Information Technology Services, the University of Hong Kong.

CONFLICT OF INTEREST

The authors report no conflict of interest.

DATA AVAILABILITY STATEMENT

The research data associated with this article are included in the article.

REFERENCES

[1] G.D. Akrivis, V.A. Dougalis and O.A. Karakashian, On fully discrete Galerkin methods of second-order temporal accuracy for the nonlinear Schrödinger equation. *Numer. Math.* **59** (1991) 31–53.

[2] R. Altmann, P. Henning and D. Peterseim, Numerical homogenization beyond scale separation. *Acta Numer.* **30** (2021) 1–86.

[3] X. Antoine, W. Bao and C. Besse, Computational methods for the dynamics of the nonlinear Schrödinger/Gross–Pitaevskii equations. *Comput. Phys. Comm.* **184** (2013) 2621–2633.
[4] W. Auzinger, T. Kassebacher, O. Koch and M. Thalhammer, Convergence of a Strang splitting finite element discretization for the Schrödinger–Poisson equation. *ESAIM: M2AN* **51** (2017) 1245–1278.
[5] W. Bao and Y. Cai, Mathematical theory and numerical methods for Bose–Einstein condensation. *Kinet. Relat. Models* **6** (2013) 1–135.
[6] W. Bao, S. Jin and P.A. Markowich, On time-splitting spectral approximations for the Schrödinger equation in the semiclassical regime. *J. Comput. Phys.* **175** (2002) 487–524.
[7] W. Bao, D. Jaksch and P.A. Markowich, Numerical solution of the Gross–Pitaevskii equation for Bose–Einstein condensation. *J. Comput. Phys.* **187** (2003) 318–342.
[8] W. Bao, S. Jin and P.A. Markowich, Numerical study of time-splitting spectral discretizations of nonlinear Schrödinger equations in the semiclassical regimes. *SIAM J. Sci. Comput.* **25** (2003) 27–64.
[9] C. Besse, A relaxation scheme for the nonlinear Schrödinger equation. *SIAM J. Numer. Anal.* **42** (2004) 934–952.
[10] C. Besse, B. Bidégaray and S. Descombes, Order estimates in time of splitting methods for the nonlinear Schrödinger equation. *SIAM J. Numer. Anal.* **40** (2003) 26–40.
[11] C. Besse, S. Descombes, G. Dujardin and I. Lacroix-Violet, Energy-preserving methods for nonlinear Schrödinger equations. *IMA J. Numer. Anal.* **41** (2020) 618–653.
[12] J. Chen, D. Ma and Z. Zhang, A multiscale finite element method for the Schrödinger equation with multiscale potentials. *SIAM J. Sci. Comput.* **41** (2019) B1115–B1136.
[13] J. Chen, S. Li and Z. Zhang, Efficient multiscale methods for the semiclassical Schrödinger equation with time-dependent potentials. *Comput. Methods Appl. Mech. Eng.* **369** (2020) 113232.
[14] J. Chen, D. Ma and Z. Zhang, A multiscale reduced basis method for the Schrödinger equation with multiscale and random potentials. *Multiscale Model. Simul.* **18** (2020) 1409–1434.
[15] E.T. Chung, Y. Efendiev and G. Li, An adaptive GMsFEM for high-contrast flow problems. *J. Comput. Phys.* **273** (2014) 54–76.
[16] S. Descombes, Convergence of a splitting method of high order for reaction–diffusion systems. *Math. Comput.* **70** (2001) 1481–1501.
[17] J. Dick, F.Y. Kuo and I.H. Sloan, High-dimensional integration: the quasi-Monte Carlo way. *Acta Numer.* **22** (2013) 133–288.
[18] C. Döding, P. Henning and J. Wärnegård, An efficient two level approach for simulating Bose–Einstein condensates. Preprint arXiv:2212.07392 (2022).
[19] S. Donsa, H. Hofstätter, O. Koch, J. Burgdörfer and I. Březinová, Long-time expansion of a Bose–Einstein condensate: observability of Anderson localization. *Phys. Rev. A* **96** (2017) 043630.
[20] W. E and B. Engquist, The heterognous multiscale methods. *Commun. Math. Sci.* **1** (2003) 87–132.
[21] Y. Efendiev, J. Galvis and T.Y. Hou, Generalized multiscale finite element methods (GMsFEM). *J. Comput. Phys.* **251** (2013) 116–135.
[22] Y. Efendiev and T.Y. Hou, Multiscale Finite Element Methods: Theory and Applications. Vol. 4. Springer Science & Business Media (2009).
[23] S. Fishman, Y. Krivolapov and A. Soffer, The nonlinear Schrödinger equation with a random potential: results and puzzles. *Nonlinearity* **25** (2012) R53.
[24] I. García-Mata and D.L. Shepelyansky, Delocalization induced by nonlinearity in systems with disorder. *Phys. Rev. E* **79** (2009) 026205.
[25] I.G. Graham, F.Y. Kuo, J.A. Nichols, R. Scheichl, C. Schwab and I.H. Sloan, Quasi-Monte Carlo finite element methods for elliptic PDEs with lognormal random coefficients. *Numer. Math.* **131** (2015) 329–368.
[26] P. Henning and A. Målqvist, Localized orthogonal decomposition techniques for boundary value problems. *SIAM J. Sci. Comput.* **36** (2014) A1609–A1634.
[27] P. Henning and A. Persson, On optimal convergence rates for discrete minimizers of the Gross–Pitaevskii energy in localized orthogonal decomposition spaces. *Multiscale Model. Simul.* **21** (2023) 993–1011.
[28] P. Henning and J. Wärnegård, Numerical comparison of mass-conservative schemes for the Gross–Pitaevskii equation. *Kinet. Relat. Models* **12** (2019) 1247–1271.
[29] P. Henning and J. Wärnegård, Superconvergence of time invariants for the Gross–Pitaevskii equation. *Math. Comput.* **91** (2022) 509–555.
[30] P. Henning, A. Målqvist and D. Peterseim, Two-level discretization techniques for ground state computations of Bose–Einstein condensates. *SIAM J. Numer. Anal.* **52** (2014) 1525–1550.

[31] T.Y. Hou and X.-H. Wu, A multiscale finite element method for elliptic problems in composite materials and porous media. *J. Comput. Phys.* **134** (1997) 169–189.
[32] T.Y. Hou and P. Zhang, Sparse operator compression of higher-order elliptic operators with rough coefficients. *Res. Math. Sci.* **4** (2017) 24.
[33] T. Hou, P. Liu and Z. Zhang, A model reduction method for elliptic PDEs with random input using the heterogeneous stochastic FEM framework. *Bull. Inst. Math.* **11** (2016) 179–216.
[34] T.Y. Hou, D. Ma and Z. Zhang, A model reduction method for multiscale elliptic PDEs with random coefficients using an optimization approach. *Multiscale Model. Simul.* **17** (2019) 826–853.
[35] A. Iomin, Subdiffusion in the nonlinear Schrödinger equation with disorder. *Phys. Rev. E* **81** (2010) 017601.
[36] K. Karhunen, Über lineare methoden in der wahrscheinlichkeitsrechnung. *Annales Academiae Scientiarum Fennicae: Ser. A* **37** (1947) 1.
[37] M. Knöller, A. Ostermann and K. Schratz, A Fourier integrator for the cubic nonlinear Schrödinger equation with rough initial data. *SIAM J. Numer. Anal.* **57** (2019) 1967–1986.
[38] S. Li and Z. Zhang, Computing eigenvalues and eigenfunctions of Schrödinger equations using a model reduction approach. *Commun. Comput. Phys.* **24** (2018) 1073–1100.
[39] S. Li, Z. Zhang and H. Zhao, A data-driven approach for multiscale elliptic PDEs with random coefficients based on intrinsic dimension reduction. *Multiscale Model. Simul.* **18** (2020) 1242–1271.
[40] M. Loève, Probability Theory II. Vol. 46 of *Graduate Texts in Mathematics* (1978).
[41] J.C. López-Marcos and J.M. Sanz-Serna, A definition of stability for nonlinear problems. *Numer. Treatment Differ. Equ.* **104** (1988) 216–226.
[42] D. Ma and Z. Zhang, A quasi monte carlo-based model reduction method for solving Helmholtz equation in random media. *Commun. Anal. Comput. (CAC)* **1** (2023). DOI: 10.3934/cac.2023015.
[43] A. Målqvist and D. Peterseim, Computation of eigenvalues by numerical upscaling. *Numer. Math.* **130** (2015) 337–361.
[44] A. Målqvist and D. Peterseim, Numerical Homogenization by Localized Orthogonal Decomposition. Society for Industrial and Applied Mathematics, Philadelphia, PA (2020).
[45] M. Meister, S. Arnold, D. Moll, M. Eckart, E. Kajari, M.A. Efremov, R. Walser and W.P. Schleich, Chapter six – Efficient description of Bose–Einstein condensates in time-dependent rotating traps, in Advances in Atomic, Molecular, and Optical Physics. Vol. 66. Academic Press (2017) 375–438.
[46] A.V. Milovanov and A. Iomin, Destruction of Anderson localization in quantum nonlinear Schrödinger lattices. *Phys. Rev. E* **95** (2017) 042142.
[47] A. Ostermann, Y. Wu and F. Yao, A second-order low-regularity integrator for the nonlinear Schrödinger equation. *Adv. Contin. Discrete Models* **2022** (2022) 1–14.
[48] H. Owhadi, Multigrid with rough coefficients and multiresolution operator decomposition from hierarchical information games. *SIAM Rev.* **59** (2017) 99–149.
[49] H. Owhadi and L. Zhang, Localized bases for finite-dimensional homogenization approximations with nonseparated scales and high contrast. *Multiscale Model. Simul.* **9** (2011) 1373–1398.
[50] D. Peterseim, Eliminating the pollution effect in Helmholtz problems by local subspace correction. *Math. Comput.* **86** (2017) 1005–1036.
[51] A.S. Pikovsky and D.L. Shepelyansky, Destruction of Anderson localization by a weak nonlinearity. *Phys. Rev. Lett.* **100** (2008) 094101.
[52] J.M. Sanz-Serna, Methods for the numerical solution of the nonlinear Schrödinger equation. *Math. Comput.* **43** (1984) 21–27.
[53] C. Schwab and R.A. Todor, Karhunen–Loéve approximation of random fields by generalized fast multipole methods. *J. Comput. Phys.* **217** (2006) 100–122.
[54] D.L. Shepelyansky, Delocalization of quantum chaos by weak nonlinearity. *Phys. Rev. Lett.* **70** (1993) 1787–1790.
[55] M.E. Taylor, Partial Differential Equations III: Nonlinear Equations. *Applied Mathematical Sciences*. Springer New York (2010).
[56] M. Thalhammer, High-order exponential operator splitting methods for time-dependent Schrödinger equations. *SIAM J. Numer. Anal.* **46** (2008) 2022–2038.
[57] J. Wang, A new error analysis of Crank-Nicolson Galerkin FEMs for a generalized nonlinear Schrödinger equation. *J. Sci. Comput.* **60** (2014) 390–407.
[58] Z. Wang, X. Luo, S. Yau and Z. Zhang, Proper orthogonal decomposition method to nonlinear filtering problems in medium-high dimension. *IEEE Trans. Autom. Control* **65** (2019) 1613–1624.

[59] Z. Wu and Z. Zhang, Convergence analysis of the localized orthogonal decomposition method for the semiclassical Schrödinger equations with multiscale potentials. *J. Sci. Comput.* **93** (2022) 73.
[60] Z. Wu, Z. Zhang and X. Zhao, Error estimate of a quasi-Monte Carlo time-splitting pseudospectral method for nonlinear Schrödinger equation with random potentials. *SIAM/ASA J. Uncertainty Quantif.* **12** (2024) 1–29.
[61] X. Zhao, Numerical integrators for continuous disordered nonlinear Schrödinger equation. *J. Sci. Comput.* **89** (2021) 40.
[62] G.E. Zouraris, On the convergence of a linear two-step finite element method for the nonlinear Schrödinger equation. *ESAIM: M2AN* **35** (2001) 389–405.

Appendix A. A multiscale reduced basis method

As a supplement, we present an approach to reduce the computational effort required for construction basis functions for random potentials. This approach is motivated by the method proposed in [14, 39, 58], which consists of offline and online stages. In the offline stage, let $\{v(\boldsymbol{x},\omega_q)\}_{q=1}^{Q}$ be the samples of potential with Q representing the number of samples. At the node $\boldsymbol{x}_p$, the sample mean of multiscale basis functions is given by $\zeta_p^0 = \frac{1}{Q}\sum_{q=1}^{Q}\phi_p(\boldsymbol{x},\omega_q)$, and the fluctuation is defined as $\tilde{\phi}_p(\boldsymbol{x},\omega_q) = \phi_p(\boldsymbol{x},\omega_q) - \zeta_p^0$. We employ the POD method on $\{\tilde{\phi}_p(\boldsymbol{x},\omega_q)\}_{q=1}^{Q}$ to build a set of reduced basis functions $\{\zeta_p^1(\boldsymbol{x}),\cdots,\zeta_p^{m_p}(\boldsymbol{x})\}$ with $m_p \ll Q$. In the online stage, the multiscale basis function at $\boldsymbol{x}_p$ has the following form

$$\phi_p(\boldsymbol{x},\omega) = \sum_{l=0}^{m_p} c_p^l(\omega)\zeta_p^l(\boldsymbol{x}), \tag{A.1}$$

where $\{c_p^l\}_{l=0}^{m_p}$ are unknowns. Due to the wave function being represented by

$$\psi_H^\epsilon(\boldsymbol{x},t,\omega) = \sum_{p=1}^{N_H}\sum_{l=0}^{m_p} c_p^l(t,\omega)\zeta_p^l(\boldsymbol{x}), \tag{A.2}$$

the dofs in the Galerkin formulation is $\sum_{p=1}^{N_H}(m_p+1)$. To reduce the dofs of the Galerkin formulation, we compute $\{c_p^l\}_{l=0}^{m_p}$ in (A.1) by solving the following reduced optimal problems

$$\min\ a(\phi_p,\phi_p), \tag{A.3}$$

$$\text{s.t.}\ \int_{\mathcal{D}} \phi_p\phi_q^H\,\mathrm{d}\mathbf{x} = \lambda(H)\delta_{pq}, \quad \forall 1 \le q \le N_H. \tag{A.4}$$

We remark that the above optimal problems need to be solved for all realizations of random potentials in the online stage. Since the value of m_p is small [14], the computation cost of constructing the multiscale basis functions can be reduced, while the dofs in the Galerkin formulation remain at N_H in the online stage. In addition, we adopt parallel implementations with 12 cores in the following tests.

To demonstrate the improvement offered by the reduced multiscale basis method, we carry out two numerical tests. We fix $m_p = 3$ for $p = 1,\cdots,N_H$, and generate 1000 samples using the qMC method, with 200 samples allocated for the offline stage and the remaining 800 samples used in the online stage. The **SI** method is employed for time evolution.

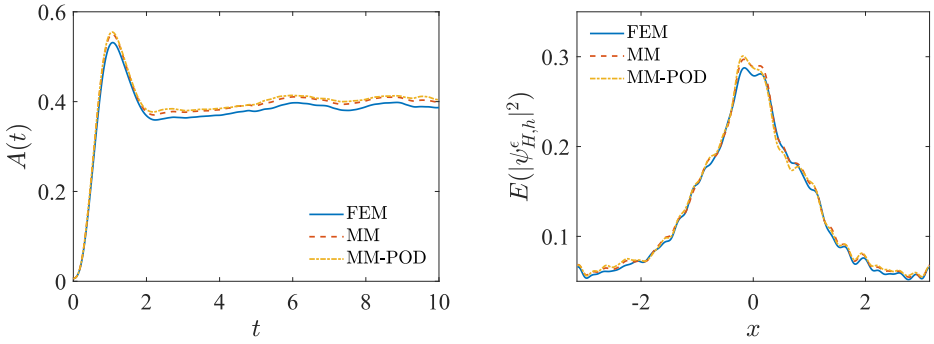

FIGURE A.1. Numerical comparison of the FEM, the multiscale method (MM), and the MM-POD method.

TABLE A.1. Comparison of time costs (second) for the FEM, MM, and MM-POD methods.

Sample number	FEM	MM	MM-POD (offline)
1000	2116	152	107 (35)
2000	4205	308	243 (35)
4000	8376	620	501 (34)
8000	16 633	1239	1020 (40)
16 000	33 469	2466	2137 (43)

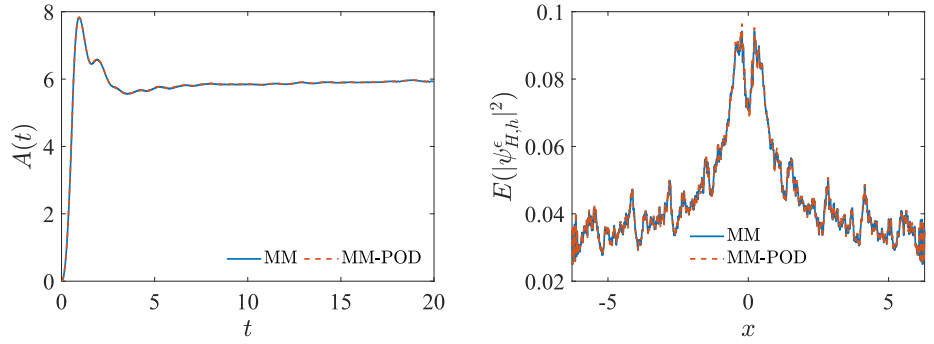

FIGURE A.2. Numerical comparison of the direct multiscale method (MM) and the MM-POD method for the 1D NLSE with $\lambda = 20$.

We compare the numerical solution computed by the FEM, the multiscale method, and the multiscale POD (MM-POD) reduction method as in Figure A.1.

Furthermore, we vary the qMC samples and record the corresponding time costs in Table A.1. Note that the time costs of MM-POD method are attributed to both the offline and online stages of the computations. As illustrated in Table A.1, a considerable enhancement in simulation efficiency is achieved through the application of the multiscale method, with additional improvements attained in the integration of the POD reduction method.

We further carry out an experiment of NLSE with $\lambda = 20$. The corresponding numerical results are shown in Figure A.2. The MM-POD method takes approximately 14 978 s (4.16 h), with 1064 s spent on the offline stage. In contrast, the direct multiscale method takes 20 061 s (5.57 h).

Appendix B. The proof of Lemma 2.1

Proof. We first study the regularity of ψ^ϵ in space. Since the energy is a constant

$$E(t) = \frac{\epsilon^2}{2}\|\nabla\psi^\epsilon\|^2 + \left(v, |\psi^\epsilon|^2\right) + \frac{\lambda}{2}\|\psi^\epsilon\|_{L^4}^4 = E_0 < \infty$$

with $\lambda \geq 0$, we directly get

$$\frac{\epsilon^2}{2}\|\nabla\psi^\epsilon\|^2 = E_0 - \left(v, |\psi^\epsilon|^2\right) - \frac{\lambda}{2}\|\psi^\epsilon\|_{L^4}^4 \leq E_0 + \|v\|_\infty,$$

which means

$$\|\nabla\psi^\epsilon\| \leq \frac{C}{\epsilon}.$$

Meanwhile, we also have

$$\|\psi^\epsilon\|_{L^4}^4 \leq \frac{E_0 + \|v\|_\infty}{\lambda}. \tag{B.1}$$

Owing to the Hamiltonian $\mathcal{H}$ is not explicitly dependent on time, and $[\mathcal{H}^2, \mathcal{H}] = 0$, the following average value of mechanics quantity is independent of time, *i.e.*,

$$\left(\mathcal{H}^2\psi^\epsilon, \psi^\epsilon\right) = E_1 \tag{B.2}$$

with $\mathrm{d}_t E_1 = 0$. Explicitly, we have

$$\begin{aligned}\left(\mathcal{H}^2\psi^\epsilon, \psi^\epsilon\right) = {}& \frac{\epsilon^4}{4}\left(\Delta^2\psi^\epsilon, \psi^\epsilon\right) + \left(v^2\psi^\epsilon, \psi^\epsilon\right) + \lambda^2\left(|\psi^\epsilon|^4\psi^\epsilon, \psi^\epsilon\right) \\ & - \epsilon^2(\Delta v\psi^\epsilon, \psi^\epsilon) + 2\lambda\left(v|\psi^\epsilon|^2\psi^\epsilon, \psi^\epsilon\right) - \lambda\epsilon^2\left(\Delta|\psi^\epsilon|^2\psi^\epsilon, \psi^\epsilon\right).\end{aligned}$$

We then get

$$\begin{aligned}\frac{\epsilon^4}{4}\|\Delta\psi^\epsilon\|^2 + \|v\psi^\epsilon\|^2 + \lambda^2\|\psi^\epsilon\|_{L^6}^6 &\leq E_1 + \epsilon^2(\Delta v\psi^\epsilon, \psi^\epsilon) - 2\lambda\left(v|\psi^\epsilon|^2\psi^\epsilon, \psi^\epsilon\right) + \lambda\epsilon^2\left(\Delta|\psi^\epsilon|^2\psi^\epsilon, \psi^\epsilon\right) \\ &\leq E_1 - \epsilon^2(\nabla v\psi^\epsilon, \nabla\psi^\epsilon) + 2\lambda\|v\|_\infty\|\psi^\epsilon\|_{L^4}^4 + 3\lambda\epsilon^2\|\psi^\epsilon\|_\infty^2\|\nabla\psi^\epsilon\|^2 \\ &\leq E_1 + C\|v\|_\infty + \epsilon\|\nabla v\|_\infty + 2\lambda\|v\|_\infty\|\psi^\epsilon\|_{L^4}^4 + 3\lambda C\|\psi^\epsilon\|_\infty^2.\end{aligned}$$

Hence, there exists a constant C that depends on $\|v\|_\infty$, $\|\nabla v\|_\infty$, E_0, E_1, and $\|\psi^\epsilon\|_\infty$ such that

$$\left\|\nabla^2\psi^\epsilon\right\| \leq \frac{C}{\epsilon^2}, \quad \|\psi^\epsilon\|_{L^6}^6 \leq \frac{C}{\lambda^2}. \tag{B.3}$$

Furthermore, if $\psi^\epsilon \in H^4$, we also have $[\mathcal{H}^s, \mathcal{H}] = 0$ for $s \leq 4$. Repeat the above procedures and we can get

$$\|\nabla^s\psi^\epsilon\| \leq \frac{C}{\epsilon^s}. \tag{B.4}$$

Next, we study the bound of $\|\partial_t\psi^\epsilon\|_{H^s}$ with $0 \leq s \leq 2$. Taking the time derivative for (2.1) yields

$$i\epsilon\partial_{tt}\psi^\epsilon = -\frac{\epsilon^2}{2}\Delta\partial_t\psi^\epsilon + v\partial_t\psi^\epsilon + 2\lambda|\psi^\epsilon|^2\partial_t\psi^\epsilon + \lambda(\psi^\epsilon)^2\partial_t\bar{\psi}^\epsilon. \tag{B.5}$$

Take inner product of this equation with $\partial_t\psi^\epsilon$ and we get

$$i\epsilon\,\mathrm{d}_t(\partial_t\psi^\epsilon, \partial_t\psi^\epsilon) = \lambda\int_{\mathcal{D}}\left(\partial_t\psi^\epsilon\bar{\psi}^\epsilon\right)^2 - \left(\partial_t\bar{\psi}^\epsilon\psi^\epsilon\right)^2\mathrm{d}\boldsymbol{x} = 4i\lambda\int_{\mathcal{D}}\Re\left(\partial_t\psi^\epsilon\bar{\psi}^\epsilon\right)\Im\left(\partial_t\psi^\epsilon\bar{\psi}^\epsilon\right)\mathrm{d}\boldsymbol{x}. \tag{B.6}$$

Thus we have

$$\epsilon\,\mathrm{d}_t\|\partial_t\psi^\epsilon\|^2 \leq 2\lambda\|\partial_t\psi^\epsilon\psi^\epsilon\|^2 \leq 2\lambda\|\psi^\epsilon\|_\infty^2\|\partial_t\psi^\epsilon\|^2,$$

which indicates

$$\|\partial_t\psi^\epsilon\| \le \|\partial_t\psi_{\rm in}\| \exp\left(\frac{2\lambda T\|\psi^\epsilon\|_\infty^2}{\epsilon}\right). \tag{B.7}$$

For the initial condition, we have

$$\|\partial_t\psi_{\rm in}\| \le \frac{\epsilon}{2}\|\nabla\psi_{\rm in}\| + \frac{1}{\epsilon}(v\psi_{\rm in},\psi_{\rm in}) + \frac{\lambda}{\epsilon}\|\psi_{\rm in}\|_{L^4}^2 \le \frac{C}{\epsilon}.$$

We therefore get

$$\|\partial_t\psi^\epsilon\| \le \frac{C}{\epsilon}\exp\left(\frac{2\lambda\|\psi^\epsilon\|_\infty^2 T}{\epsilon}\right). \tag{B.8}$$

Take inner product of the equation (B.5) with $\partial_t\Delta\psi^\epsilon$, and we have

$$\begin{aligned}\epsilon\,\mathrm{d}_t\|\nabla\partial_t\psi^\epsilon\|^2 = \Im\Big\{&2(\nabla v\partial_t\psi^\epsilon,\nabla\partial_t\psi^\epsilon) + 4\lambda\big(\psi^\epsilon\partial_t\psi^\epsilon\nabla\bar\psi^\epsilon,\nabla\partial_t\psi^\epsilon\big)\\ &+ 4\lambda\big(\bar\psi^\epsilon\partial_t\psi^\epsilon\nabla\psi^\epsilon,\nabla\partial_t\psi^\epsilon\big) + 4\lambda(\psi^\epsilon\partial_t\psi^\epsilon\nabla\psi^\epsilon,\nabla\partial_t\psi^\epsilon) + 2\lambda\Big((\psi^\epsilon)^2,(\nabla\partial_t\psi^\epsilon)^2\Big)\Big\}.\end{aligned}$$

By the inequalities

$$\begin{aligned}\|\psi^\epsilon\partial_t\psi^\epsilon\nabla\psi^\epsilon\nabla\partial_t\psi^\epsilon\|_{L^1} &\le \|\psi^\epsilon\|_{L^6}\|\partial_t\psi^\epsilon\|_{L^6}\|\nabla\psi^\epsilon\|_{L^6}\|\nabla\partial_t\psi^\epsilon\|\\ &\le C\|\psi^\epsilon\|_{L^6}\left(\frac{d}{3}\|\partial_t\nabla\psi^\epsilon\| + \left(1-\frac{d}{3}\right)\|\partial_t\psi^\epsilon\|\right)\big\|\nabla^2\psi^\epsilon\big\|^{\frac12+\frac{d}{6}}\|\nabla\partial_t\psi^\epsilon\|\\ &\le C\|\psi^\epsilon\|_{L^6}(\|\partial_t\nabla\psi^\epsilon\| + \|\partial_t\psi^\epsilon\|)\big\|\nabla^2\psi^\epsilon\big\|\|\nabla\partial_t\psi^\epsilon\|\end{aligned}$$

and

$$\Big\|(\psi^\epsilon)^2(\nabla\partial_t\psi^\epsilon)^2\Big\|_{L^1} \le \|\psi^\epsilon\|_{L^\infty}^2\|\nabla\partial_t\psi^\epsilon\|^2,$$

we get

$$\epsilon\,\mathrm{d}_t\|\partial_t\nabla\psi^\epsilon\| \le 2\|\nabla v\|_\infty\|\partial_t\psi^\epsilon\| + C\lambda\big\|\nabla^2\psi^\epsilon\big\|(\|\partial_t\nabla\psi^\epsilon\| + \|\partial_t\psi^\epsilon\|) + 2\lambda\|\psi^\epsilon\|_{L^\infty}^2\|\nabla\partial_t\psi^\epsilon\|.$$

Then we arrive at

$$\begin{aligned}\|\partial_t\nabla\psi^\epsilon\| &\le \left(\frac{2\|\nabla v\|_\infty}{\epsilon} + \frac{C\lambda\big\|\nabla^2\psi^\epsilon\big\|}{\epsilon}\right)\|\partial_t\psi^\epsilon\|\exp\left(\frac{C\lambda T\big\|\nabla^2\psi^\epsilon\big\|}{\epsilon} + \frac{2\lambda T\|\psi^\epsilon\|_\infty^2}{\epsilon}\right)\\ &\le \frac{C\lambda}{\epsilon^4}\exp\left(\frac{C\lambda T}{\epsilon^3}\right).\end{aligned}$$

Let $d=3$, and the above result can be replaced with

$$\|\partial_t\nabla\psi^\epsilon\| \le \frac{2\|\nabla v\|_\infty}{\epsilon}\|\partial_t\psi^\epsilon\|\exp\left(\frac{C\lambda T\big\|\nabla^2\psi^\epsilon\big\|}{\epsilon} + \frac{2\lambda T\|\psi^\epsilon\|_\infty^2}{\epsilon}\right). \tag{B.9}$$

By the similar procedures, we have

$$\begin{aligned}\epsilon\,\mathrm{d}_t\big\|\partial_t\nabla^2\psi^\epsilon\big\|^2 \le{}& \big\|\nabla^2 v\big\|_\infty\|\partial_t\psi^\epsilon\|\big\|\partial_t\nabla^2\psi^\epsilon\big\| + 2\|\nabla v\|_\infty\|\partial_t\nabla\psi^\epsilon\|\big\|\partial_t\nabla^2\psi^\epsilon\big\|\\ &+ C\lambda\big\|\nabla^3\psi^\epsilon\big\|^{\frac23+\frac{d}{9}}\|\partial_t\nabla\psi^\epsilon\|^{\frac{d}{3}}\|\partial_t\psi^\epsilon\|^{1-\frac{d}{3}}\big\|\partial_t\nabla^2\psi^\epsilon\big\|\\ &+ C\lambda\big\|\nabla^3\psi^\epsilon\big\|^{\frac{6}{9-d}}\|\psi^\epsilon\|_{L^6}^{2-\frac{6}{9-d}}\|\partial_t\nabla\psi^\epsilon\|^{\frac{d}{3}}\|\partial_t\psi^\epsilon\|^{1-\frac{d}{3}}\big\|\partial_t\nabla^2\psi^\epsilon\big\|\\ &+ C\lambda\big\|\nabla^2\psi^\epsilon\big\|^{\frac12+\frac{d}{6}}\big\|\partial_t\nabla^2\psi^\epsilon\big\|^{\frac12+\frac{d}{6}}\|\partial_t\psi^\epsilon\|^{\frac12-\frac{d}{6}}\big\|\partial_t\nabla^2\psi^\epsilon\big\| + C\lambda\|\psi^\epsilon\|_\infty^2\big\|\partial_t\nabla^2\psi^\epsilon\big\|^2\end{aligned}$$

in which we use the inequalities

$$\begin{aligned}
\big\|\nabla^2\psi^\epsilon\psi^\epsilon\partial_t\psi^\epsilon\partial_t\nabla^2\psi^\epsilon\big\|_{L^1} &\le \|\psi^\epsilon\|_{L^6}\big\|\nabla^2\psi^\epsilon\big\|_{L^6}\|\partial_t\psi^\epsilon\|_{L^6}\big\|\partial_t\nabla^2\psi^\epsilon\big\|\\
&\le C\big\|\nabla^3\psi^\epsilon\big\|^{\frac{2}{3}+\frac{d}{9}}\|\partial_t\nabla\psi^\epsilon\|^{\frac{d}{3}}\|\partial_t\psi^\epsilon\|^{1-\frac{d}{3}}\big\|\partial_t\nabla^2\psi^\epsilon\big\|,\\
\big\|\nabla\psi^\epsilon\nabla\psi^\epsilon\partial_t\psi^\epsilon\partial_t\nabla^2\psi^\epsilon\big\|_{L^1} &\le \|\nabla\psi^\epsilon\|_{L^6}^2\|\partial_t\psi^\epsilon\|_{L^6}\big\|\partial_t\nabla^2\psi^\epsilon\big\|\\
&\le C\big\|\nabla^3\psi^\epsilon\big\|^{\frac{6}{9-d}}\|\psi^\epsilon\|_{L^6}^{2-\frac{6}{9-d}}\|\partial_t\nabla\psi^\epsilon\|^{\frac{d}{3}}\|\partial_t\psi^\epsilon\|^{1-\frac{d}{3}}\big\|\partial_t\nabla^2\psi^\epsilon\big\|,\\
\big\|\psi^\epsilon\nabla\psi^\epsilon\partial_t\nabla\psi^\epsilon\partial_t\nabla^2\psi^\epsilon\big\|_{L^1} &\le \|\psi^\epsilon\|_{L^6}\|\nabla\psi^\epsilon\|_{L^6}\|\partial_t\nabla\psi^\epsilon\|_{L^6}\big\|\partial_t\nabla^2\psi^\epsilon\big\|\\
&\le C\big\|\nabla^2\psi^\epsilon\big\|^{\frac{1}{2}+\frac{d}{6}}\big\|\partial_t\nabla^2\psi^\epsilon\big\|^{\frac{1}{2}+\frac{d}{6}}\|\partial_t\psi^\epsilon\|^{\frac{1}{2}-\frac{d}{6}}\big\|\partial_t\nabla^2\psi^\epsilon\big\|,
\end{aligned}$$

and

$$\Big\|(\psi^\epsilon)^2\big(\partial_t\nabla^2\psi^\epsilon\big)\Big\|_{L^1} \le \|\psi^\epsilon\|_\infty^2\big\|\partial_t\nabla^2\psi^\epsilon\big\|^2.$$

Then we get

$$\big\|\partial_t\nabla^2\psi^\epsilon\big\| \le \frac{C\lambda\big\|\nabla^3\psi^\epsilon\big\|^\ell\|\partial_t\nabla\psi^\epsilon\|^{\frac{d}{3}}\|\partial_t\psi^\epsilon\|^{1-\frac{d}{3}}}{\epsilon}\exp\left(\frac{C\lambda T\big\|\nabla^2\psi^\epsilon\big\|+C\lambda T\|\psi^\epsilon\|_\infty^2}{\epsilon}\right), \tag{B.10}$$

where $\ell=\max\{\frac{2}{3}+\frac{d}{9},\frac{6}{9-d}\}$. Let $d=3$ and we get the compact form

$$\big\|\partial_t\nabla^2\psi^\epsilon\big\| \le \frac{C\lambda\big\|\nabla^3\psi^\epsilon\big\|}{\epsilon}\|\partial_t\nabla\psi^\epsilon\|\exp\left(\frac{C\lambda T\big\|\nabla^2\psi^\epsilon\big\|+C\lambda T\|\psi^\epsilon\|_\infty^2}{\epsilon}\right). \tag{B.11}$$

Due to $\epsilon\ll 1$, the order of $\|\partial_t\psi^\epsilon\|_{H^s}$ with respect to ϵ directly depends on the estimate $\|\partial_t\nabla^s\psi^\epsilon\|$. Thus, there exists a constant $C_{\lambda,\epsilon}$ that depends on λ and ϵ such that $\|\partial_t\psi^\epsilon\|_{H^s}\le C_{\lambda,\epsilon}$. This completes the proof. □

Appendix C. The proof of Lemma 4.4

Proof. Let $|\boldsymbol{\nu}|=1$, and we take the derivative with respect to $\xi_j(\omega)$ of (2.10). Denote $\partial_j\psi_m=\partial_{\xi_j}\psi_m^\epsilon$ and $\partial_j v_m=\partial_{\xi_j}v_m^\epsilon$, and we get

$$i\epsilon\partial_t(\partial_j\psi_m)=-\frac{\epsilon^2}{2}\Delta(\partial_j\psi_m)+(\partial_j v_m)\psi_m^\epsilon+v_m^\epsilon(\partial_j\psi_m)+\lambda\Big(2|\psi_m^\epsilon|^2\partial_j\psi_m+(\psi_m^\epsilon)^2\partial_j\bar\psi_m\Big).$$

We have

$$\begin{aligned}
\epsilon\,\mathrm{d}_t\|\partial_j\psi_m\| &\le 2\|\partial_j v_m\|_\infty+2\lambda\|\psi_m^\epsilon\|_\infty^2\|\partial_j\psi_m\|,\\
\epsilon\,\mathrm{d}_t\|\nabla\partial_j\psi_m\| &\le 2\|\nabla\partial_j v_m\|_\infty+2\|\partial_j v_m\|_\infty\|\nabla\psi_m^\epsilon\|+2\|\nabla v_m\|_\infty\|\partial_j\psi_m\|\\
&\quad+16\lambda\|\psi_m^\epsilon\|_\infty\|\partial_j\psi_m\|_{L^4}\|\nabla\psi_m^\epsilon\|_{L^4}+2\lambda\|\psi_m^\epsilon\|_\infty^2\|\nabla\partial_j\psi_m\|,\\
\epsilon\,\mathrm{d}_t\|\nabla^2\partial_j\psi_m\| &\le 2\|\nabla^2\partial_j v_m\|_\infty+4\|\nabla\partial_j v_m\|_\infty\|\nabla\psi_m^\epsilon\|+2\|\partial_j v_m\|_\infty\|\nabla^2\psi_m^\epsilon\|\\
&\quad+2\|\nabla^2 v_m\|_\infty\|\partial_j\psi_m\|+4\|\nabla v_m\|_\infty\|\nabla\partial_j\psi_m\|+8\lambda\|\psi_m^\epsilon\|_\infty\|\nabla^2\psi_m^\epsilon\|_{L^4}\|\partial_j\psi_m\|_{L^4}\\
&\quad+8\lambda\|\nabla\psi_m^\epsilon\|_{L^6}^2\|\partial_j\psi_m\|_{L^6}+16\lambda\|\psi_m^\epsilon\|_\infty\|\nabla\psi_m^\epsilon\|_{L^4}\|\nabla\partial_j\psi_m^\epsilon\|_{L^4}+2\lambda\|\psi_m^\epsilon\|_\infty^2\big\|\nabla^2\partial_j\psi_m\big\|.
\end{aligned}$$

Owing to

$$\begin{aligned}
\|\partial_j\psi_m\|_{L^4}\|\nabla\psi_m^\epsilon\|_{L^4} &\le C\|\nabla\partial_j\psi_m\|^{\frac{d}{4}}\|\partial_j\psi_m\|^{1-\frac{d}{4}}\|\psi_m\|_{H^2}^{\frac{1}{2}}\|\psi_m\|_\infty^{\frac{1}{2}}\\
&\le C\|\psi_m\|_{H^2}^{\frac{1}{2}}\|\psi_m\|_\infty^{\frac{1}{2}}\left(\frac{d}{4}\|\nabla\partial_j\psi_m\|+\left(1-\frac{d}{4}\right)\|\partial_j\psi_m\|\right),\\
\|\nabla^2\psi_m^\epsilon\|_{L^4}\|\partial_j\psi_m\|_{L^4} &\le C\|\nabla^3\psi_m\|^{\frac{8+d}{12}}\|\psi_m\|^{\frac{4-d}{12}}\left(\frac{d}{4}\|\nabla\partial_j\psi_m\|+\left(1-\frac{d}{4}\right)\|\partial_j\psi_m\|\right),\\
\|\nabla\psi_m^\epsilon\|_{L^6}^2\|\partial_j\psi_m\|_{L^6} &\le C\|\nabla^2\psi_m^\epsilon\|^{1+\frac{d}{3}}\|\psi^\epsilon\|^{1-\frac{d}{3}}\|\nabla\partial_j\psi_m\|^{\frac{d}{3}}\|\partial_j\psi_m\|^{1-\frac{d}{3}}\\
&\le C\|\nabla^2\psi_m^\epsilon\|^{1+\frac{d}{3}}\|\psi^\epsilon\|^{1-\frac{d}{3}}\left(\frac{d}{3}\|\nabla\partial_j\psi_m\|+\left(1-\frac{d}{3}\right)\|\partial_j\psi_m\|\right),
\end{aligned}$$

and

$$\begin{aligned}\|\nabla\psi_m^\epsilon\|_{L^4}\|\nabla\partial_j\psi_m^\epsilon\|_{L^4}&\le C\|\psi_m\|_{H^2}^{\frac12}\|\psi_m\|_\infty^{\frac12}\|\nabla^2\partial_j\psi_m\|^{\frac12+\frac{d}{8}}\|\partial_j\psi_m\|^{\frac12-\frac{d}{8}}\\&\le C\|\psi_m\|_{H^2}^{\frac12}\|\psi_m\|_\infty^{\frac12}\bigg(\Big(\frac12+\frac{d}{8}\Big)\|\nabla^2\partial_j\psi_m\|+\Big(\frac12-\frac{d}{8}\Big)\|\partial_j\psi_m\|\bigg).\end{aligned}$$

We can construct

$$\epsilon\,\mathrm{d}_t\|\partial_j\psi_m\|_{H^2}\le\frac{C_1}{\epsilon^2}\|\partial_j v_m\|_{H^2}+\frac{C_2}{\epsilon^4}\|\partial_j\psi_m\|_{H^2}.$$

Then we get for all $t\in(0,T]$

$$\|\partial_j\psi_m\|_{H^2}\le\frac{C_1t}{\epsilon^3}\|\partial_j v_m\|_{H^2}\exp\bigg(\frac{C_2t}{\epsilon^4}\bigg)\le C(t,\lambda,\epsilon,|\boldsymbol{\nu}|)\sqrt{\lambda_j}\|v_j\|_{H^2},$$

where $C(t,\lambda,\epsilon,|\boldsymbol{\nu}|)$ depends on t,λ,ϵ but is independent of dimensions.

Then for $|\boldsymbol{\nu}|\ge2$, by the Leibniz rule we have

$$\begin{aligned}i\epsilon\partial_t\partial^{\boldsymbol{\nu}}\psi_m^\epsilon&=-\frac{\epsilon^2}{2}\Delta(\partial^{\boldsymbol{\nu}}\psi_m^\epsilon)+\sum_{\boldsymbol{\mu}\preceq\boldsymbol{\nu}}\binom{\boldsymbol{\nu}}{\boldsymbol{\mu}}\partial^{\boldsymbol{\nu}-\boldsymbol{\mu}}v_m\partial^{\boldsymbol{\mu}}\psi_m^\epsilon+\lambda\sum_{\boldsymbol{\mu}\preceq\boldsymbol{\nu}}\binom{\boldsymbol{\nu}}{\boldsymbol{\mu}}\partial^{\boldsymbol{\nu}-\boldsymbol{\mu}}|\psi_m^\epsilon|^2\partial^{\boldsymbol{\mu}}\psi_m^\epsilon\\&=-\frac{\epsilon^2}{2}\Delta(\partial^{\boldsymbol{\nu}}\psi_m^\epsilon)+v_m\partial^{\boldsymbol{\nu}}\psi_m^\epsilon+\lambda\Big(2|\psi_m^\epsilon|^2\partial^{\boldsymbol{\nu}}\psi_m^\epsilon+(\psi_m^\epsilon)^2\partial^{\boldsymbol{\nu}}\bar\psi_m^\epsilon\Big)\\&\quad+\sum_{\substack{\boldsymbol{\mu}\prec\boldsymbol{\nu},\\|\boldsymbol{\nu}-\boldsymbol{\mu}|=1}}\binom{\boldsymbol{\nu}}{\boldsymbol{\mu}}\partial^{\boldsymbol{\nu}-\boldsymbol{\mu}}v_m\partial^{\boldsymbol{\mu}}\psi_m^\epsilon+\lambda\sum_{\boldsymbol{\mu}\prec\boldsymbol{\nu}}\binom{\boldsymbol{\nu}}{\boldsymbol{\mu}}\sum_{\boldsymbol{\eta}\preceq\boldsymbol{\nu}-\boldsymbol{\mu}}\binom{\boldsymbol{\nu}-\boldsymbol{\mu}}{\boldsymbol{\eta}}\partial^{\boldsymbol{\nu}-\boldsymbol{\mu}-\boldsymbol{\eta}}\psi_m^\epsilon\partial^{\boldsymbol{\mu}}\bar\psi_m^\epsilon\partial^{\boldsymbol{\eta}}\psi_m^\epsilon.\end{aligned}$$

Repeat the above procedures, and we get

$$\begin{aligned}\epsilon\,\mathrm{d}_t\|\partial^{\boldsymbol{\nu}}\psi_m^\epsilon\|&\le2|\boldsymbol{\nu}|\sum_{|\boldsymbol{\nu}-\boldsymbol{\mu}|=1}\big\|\partial^{\boldsymbol{\nu}-\boldsymbol{\mu}}v_m\big\|_\infty\|\partial^{\boldsymbol{\mu}}\psi_m^\epsilon\|+2\lambda\|\psi^\epsilon\|_\infty^2\|\partial^{\boldsymbol{\nu}}\psi_m^\epsilon\|\\&\quad+2\lambda\sum_{\boldsymbol{\mu}\prec\boldsymbol{\nu}}\binom{\boldsymbol{\nu}}{\boldsymbol{\mu}}\sum_{\boldsymbol{\eta}\preceq\boldsymbol{\nu}-\boldsymbol{\mu}}\binom{\boldsymbol{\nu}-\boldsymbol{\mu}}{\boldsymbol{\eta}}\big\|\partial^{\boldsymbol{\nu}-\boldsymbol{\mu}-\boldsymbol{\eta}}\psi_m^\epsilon\big\|_{L^6}\|\partial^{\boldsymbol{\mu}}\psi_m^\epsilon\|_{L^6}\|\partial^{\boldsymbol{\eta}}\psi_m^\epsilon\|_{L^6},\\\epsilon\,\mathrm{d}_t\|\nabla\partial^{\boldsymbol{\nu}}\psi_m^\epsilon\|&\le2\|\nabla v_m\|_\infty\|\partial^{\boldsymbol{\nu}}\psi_m\|+2\lambda C\big(\|\nabla\psi_m^\epsilon\|_{L^4}\|\partial^{\boldsymbol{\nu}}\psi_m^\epsilon\|_{L^4}+\|\nabla\partial^{\boldsymbol{\nu}}\psi_m^\epsilon\|\big)\\&\quad+2|\boldsymbol{\nu}|\sum_{|\boldsymbol{\nu}-\boldsymbol{\mu}|=1}\big(\big\|\nabla\partial^{\boldsymbol{\nu}-\boldsymbol{\mu}}v_m\big\|_\infty\|\partial^{\boldsymbol{\mu}}\psi_m^\epsilon\|+\big\|\partial^{\boldsymbol{\nu}-\boldsymbol{\mu}}v_m\big\|_\infty\|\nabla\partial^{\boldsymbol{\mu}}\psi_m^\epsilon\|\big)\\&\quad+2\lambda\sum_{\boldsymbol{\mu}\prec\boldsymbol{\nu}}\binom{\boldsymbol{\nu}}{\boldsymbol{\mu}}\sum_{\boldsymbol{\eta}\preceq\boldsymbol{\nu}-\boldsymbol{\mu}}\binom{\boldsymbol{\nu}-\boldsymbol{\mu}}{\boldsymbol{\eta}}\Big[\big\|\nabla\partial^{\boldsymbol{\nu}-\boldsymbol{\mu}-\boldsymbol{\eta}}\psi_m^\epsilon\big\|_{L^6}\|\partial^{\boldsymbol{\mu}}\psi_m^\epsilon\|_{L^6}\|\partial^{\boldsymbol{\eta}}\psi_m^\epsilon\|_{L^6}\\&\quad+\big\|\partial^{\boldsymbol{\nu}-\boldsymbol{\mu}-\boldsymbol{\eta}}\psi_m^\epsilon\big\|_{L^6}\|\nabla\partial^{\boldsymbol{\mu}}\psi_m^\epsilon\|_{L^6}\|\partial^{\boldsymbol{\eta}}\psi_m^\epsilon\|_{L^6}+\big\|\partial^{\boldsymbol{\nu}-\boldsymbol{\mu}-\boldsymbol{\eta}}\psi_m^\epsilon\big\|_{L^6}\|\partial^{\boldsymbol{\mu}}\psi_m^\epsilon\|_{L^6}\|\nabla\partial^{\boldsymbol{\eta}}\psi_m^\epsilon\|_{L^6}\Big].\end{aligned}$$

and

$$\begin{aligned}\epsilon\,\mathrm{d}_t\big\|\nabla^2\partial^{\boldsymbol{\nu}}\psi_m^\epsilon\big\|&\le2\big(\big\|\nabla^2v_m\big\|_\infty\|\partial^{\boldsymbol{\nu}}\psi_m\|+\|\nabla v_m\|_\infty\|\nabla\partial^{\boldsymbol{\nu}}\psi_m\|\big)+8\lambda\|\nabla\psi_m^\epsilon\|_{L^6}^2\|\partial^{\boldsymbol{\nu}}\psi_m\|_{L^6}\\&\quad+8\lambda\|\psi_m^\epsilon\|_\infty\big\|\nabla^2\psi_m^\epsilon\big\|_{L^4}\|\partial^{\boldsymbol{\nu}}\psi_m\|_{L^4}+16\lambda\|\psi_m^\epsilon\|_\infty\|\nabla\psi_m^\epsilon\|_{L^4}\|\nabla\partial^{\boldsymbol{\nu}}\psi_m^\epsilon\|_{L^4}\\&\quad+2|\boldsymbol{\nu}|\sum_{|\boldsymbol{\nu}-\boldsymbol{\mu}|=1}\Big[\big\|\nabla^2\partial^{\boldsymbol{\nu}-\boldsymbol{\mu}}v_m\big\|_\infty\|\partial^{\boldsymbol{\mu}}\psi_m^\epsilon\|+2\|\nabla\partial^{\boldsymbol{\nu}-\boldsymbol{\mu}}v_m\|_\infty\|\nabla\partial^{\boldsymbol{\mu}}\psi_m^\epsilon\|\\&\quad+\|\partial^{\boldsymbol{\nu}-\boldsymbol{\mu}}v_m\|_\infty\|\nabla^2\partial^{\boldsymbol{\mu}}\psi_m^\epsilon\|\Big]+2\lambda\|\psi_m^\epsilon\|_\infty^2\|\nabla^2\partial^{\boldsymbol{\nu}}\psi_m\|\\&\quad+6\lambda C\sum_{\boldsymbol{\mu}\prec\boldsymbol{\nu}}\binom{\boldsymbol{\nu}}{\boldsymbol{\mu}}\sum_{\boldsymbol{\eta}\preceq\boldsymbol{\nu}-\boldsymbol{\mu}}\binom{\boldsymbol{\nu}-\boldsymbol{\mu}}{\boldsymbol{\eta}}\|\partial^{\boldsymbol{\nu}-\boldsymbol{\mu}-\boldsymbol{\eta}}\psi_m^\epsilon\|_{H^2}\|\partial^{\boldsymbol{\mu}}\psi_m^\epsilon\|_{H^2}\|\partial^{\boldsymbol{\eta}}\psi_m^\epsilon\|_{H^2},\end{aligned}$$

in which we use the inequality generalized from Proposition 3.6 in [55] as

$$\begin{aligned}\|\nabla^2 fgh\| &\le C\|f\|_{H^2}\|g\|_{H^2}\|h\|_{H^2},\\ \|(\nabla f)(\nabla g)h\| &\le C\|f\|_{H^2}\|g\|_{H^2}\|h\|_{H^2}.\end{aligned}$$

Thus we get

$$\begin{aligned}\epsilon\,\mathrm{d}_t\|\partial^{\boldsymbol{\nu}}\psi_m^\epsilon\|_{H^2} \le{}& C_3\|\partial^{\boldsymbol{\nu}}\psi_m^\epsilon\|_{H^2} + C_4|\boldsymbol{\nu}|\sum_{|\boldsymbol{\nu}-\boldsymbol{\mu}|=1}\|\partial^{\boldsymbol{\nu}-\boldsymbol{\mu}}v_m\|_{H^2}\|\partial^{\boldsymbol{\mu}}\psi_m^\epsilon\|_{H^2}\\ &+\lambda C_5\sum_{\boldsymbol{\mu}\prec\boldsymbol{\nu}}\binom{\boldsymbol{\nu}}{\boldsymbol{\mu}}\sum_{\boldsymbol{\eta}\preceq\boldsymbol{\nu}-\boldsymbol{\mu}}\binom{\boldsymbol{\nu}-\boldsymbol{\mu}}{\boldsymbol{\eta}}\|\partial^{\boldsymbol{\nu}-\boldsymbol{\mu}-\boldsymbol{\eta}}\psi_m^\epsilon\|_{H^2}\|\partial^{\boldsymbol{\mu}}\psi_m^\epsilon\|_{H^2}\|\partial^{\boldsymbol{\eta}}\psi_m^\epsilon\|_{H^2}.\end{aligned}$$

An application of the Gronwall inequality yields

$$\begin{aligned}\|\partial^{\boldsymbol{\nu}}\psi_m^\epsilon\|_{H^2} \le{}& \exp\Big(\frac{C_3T}{\epsilon}\Big)\Big\{\frac{C_4T|\boldsymbol{\nu}|}{\epsilon}\sum_{|\boldsymbol{\nu}-\boldsymbol{\mu}|=1}\|\partial^{\boldsymbol{\nu}-\boldsymbol{\mu}}v_m\|_{H^2}\|\partial^{\boldsymbol{\mu}}\psi_m^\epsilon\|_{H^2}\\ &+\frac{\lambda C_5T}{\epsilon}\sum_{\boldsymbol{\mu}\prec\boldsymbol{\nu}}\binom{\boldsymbol{\nu}}{\boldsymbol{\mu}}\sum_{\boldsymbol{\eta}\preceq\boldsymbol{\nu}-\boldsymbol{\mu}}\binom{\boldsymbol{\nu}-\boldsymbol{\mu}}{\boldsymbol{\eta}}\|\partial^{\boldsymbol{\nu}-\boldsymbol{\mu}-\boldsymbol{\eta}}\psi_m^\epsilon\|_{H^2}\|\partial^{\boldsymbol{\mu}}\psi_m^\epsilon\|_{H^2}\|\partial^{\boldsymbol{\eta}}\psi_m^\epsilon\|_{H^2}\Big\}.\end{aligned}$$

Use the induction argument and we get

$$\|\partial^{\boldsymbol{\nu}}\psi_m\|_{H^2} \le C(t,\lambda,\epsilon,|\boldsymbol{\nu}|)\prod_j\Big(\sqrt{\lambda_j}\|v_j\|_{H^2}\Big)^{\nu_j}.$$

□